PNL-5565
UC-60

18E

Observations of Wake Characteristics at the Goodnoe Hills MOD-2 Array

J. W. Buck
D. S. Renne

August 1985

Prepared for the U.S. Department of Energy
under Contract DE-AC06-76RLO 1830

Pacific Northwest Laboratory
Operated for the U.S. Department of Energy
by Battelle Memorial Institute

Battelle

PNL-5565

DISCLAIMER

PACIFIC NORTHWEST LABORATORY
operated by
BATTELLE
for the
UNITED STATES DEPARTMENT OF ENERGY
under Contract DE-AC06-76RLO 1830

Printed in the United States of America
Available from
National Technical Information Service
United States Department of Commerce
5285 Port Royal Road
Springfield, Virginia 22161

NTIS Price Codes
Microfiche A01

Printed Copy

Pages	Price Codes
001-025	A02
026-050	A03
051-075	A04
076-100	A05
101-125	A06
126-150	A07
151-175	A08
176-200	A09
201-225	A010
226-250	A011
251-275	A012
276-300	A013

PNL-5565
UC-60

OBSERVATIONS OF WAKE CHARACTERISTICS AT THE GOODNOE HILLS MOD-2 ARRAY

J. W. Buck
D. S. Renne

August 1985

Prepared for the
U.S. Department of Energy
under Contract DE-AC06-76RLO 1830

Pacific Northwest Laboratory
Richland, Washington 99352

EXECUTIVE SUMMARY

The array of three MOD-2 wind turbines and two meteorological towers at Goodnoe Hills, Washington, provides an opportunity to evaluate turbine and wake interactions in a real environment. The triangular arrangement of the three turbines provides opportunities to study the effect of wakes on the performance of a downwind turbine at three different distances: 5, 7, and 10 rotor diameters (D), where 1 D is 300 ft. The information obtained from this test configuration is critical to future wind farm activities and is a key objective of the MOD-2 test program.

This report describes the analysis of data measured at the turbines and towers from August 29 to November 12, 1982. The data are 2-min averages of 1-s values. Background flow characteristics were also examined to determine if flow variations across the site could mask wake measurements. For this analysis, one year's data gathered at the meteorological towers were analyzed. The results show some differences between characteristics measured at the towers, but these differences were not great enough to consider in evaluating wakes at the towers.

The criterion for monitoring the effect of a wake of an upwind on a downwind machine is the power ratio of the downwind to the upwind machine. The criterion for monitoring the effect of a wake on a meteorological tower is the 200-ft wind velocity ratio of the tower in the wake to the other, free-stream, tower. These power and velocity ratios were analyzed according to wind direction, power, tip speed ratio, and turbulence intensity for the downwind distances 5, 7, and 10 D.

The results of the study show that power deficits of a downstream MOD-2 in the wake of an upstream MOD-2 average about 24% at a downwind distance of 6.7 D and 14% at a downwind distance of 10.2 D. Velocity deficits measured at the meteorological towers average 25% at 2.2 D downwind and 15% at 8.3 D downwind. Some cross-wake asymmetry and a slight curvature in the wake trajectory were observed. These effects could either be terrain-induced or the result of instrument error. Near-wake conditions were observed at 2.2 D while far-wake conditions prevailed at the other distances, with the magnitude

of the far wake smaller for higher ambient turbulence intensities. The maximum power and velocity deficits occur at a tip speed ratio of around 8, which is near the maximum C_p and C_T values of the MOD-2. There was good comparison between the averaged measured velocity deficits and those calculated by the modified Lissaman and simplified wake models, especially for higher ambient turbulence intensities.

It is recommended that the measurement program be continued so that information not available now could be examined. This information could include data describing interactions for additional turbine and tower combinations and data for different seasons, particularly spring, which is the windiest period at the site. Comparison of results of wake studies against numerical models should also be continued, so that the models can be refined to reflect actual measurements around full-scale turbines. Additional turbine parameters, such as the flapwise blade bending moment, should also be examined to determine the structural effects of wakes on downwind turbines.

CONTENTS

CONTENTS (Continued)

FIGURES

FIGURES (Continued)

FIGURES (Continued)

TABLES

OBSERVATIONS OF WAKE CHARACTERISTICS AT THE GOODNOE HILLS MOD-2 ARRAY

1.0 INTRODUCTION

1.1 BACKGROUND

In the fall of 1979, the U.S. Department of Energy (DOE) selected the Goodnoe Hills site, proposed by the Bonneville Power Administration (BPA), for the installation of a cluster of three MOD-2 wind turbine generator systems. Each MOD-2 is rated at 2500 kW. This site, selected from among twenty candidate sites proposed by utility systems around the United States, provided a unique combination of high annual average wind speeds, site accessibility, strong utility support, high public visibility, and significant opportunity for performing a variety of tests on the first cluster of large wind turbines ever to be installed.

The Goodnoe Hills site is on top of a ridge at an elevation of 2600 ft on the north side of the Columbia River. The site is approximately 20 mi east of the town of Goldendale, Washington, and approximately 120 mi east of Portland, Oregon. The terrain is relatively flat at the top, although numerous gullies cut across the site; the gullies become quite deep on both the north and the south sides. The ridge drops steeply to the river, 2200 ft below the top, on the south side and more gradually to the Goldendale valley on the north side. Vegetation at the site consists almost entirely of low sagebrush and grass, with scrub oak found in the deeper gullies to the north of the site. A computer-enhanced digitized terrain map of the site is shown in Figure 1.1.

The MOD-2 wind turbine is a two-bladed, teetering-hub, upwind machine. The rotor, which is 300 ft in diameter and weighs 50 tons, is attached to a nacelle housing the gearbox and a 2500-kW generator, and sits atop a cylindrical 200-ft high tower. Rotor speed control is accomplished by pitch control of the outer 45 ft of each blade. The machines were designed and manufactured by the Boeing Aerospace Corporation (BAC) for the DOE's Federal Wind Energy Program. The large machine development activities of the Wind Energy Program are managed by the NASA/Lewis Research Center for the DOE.

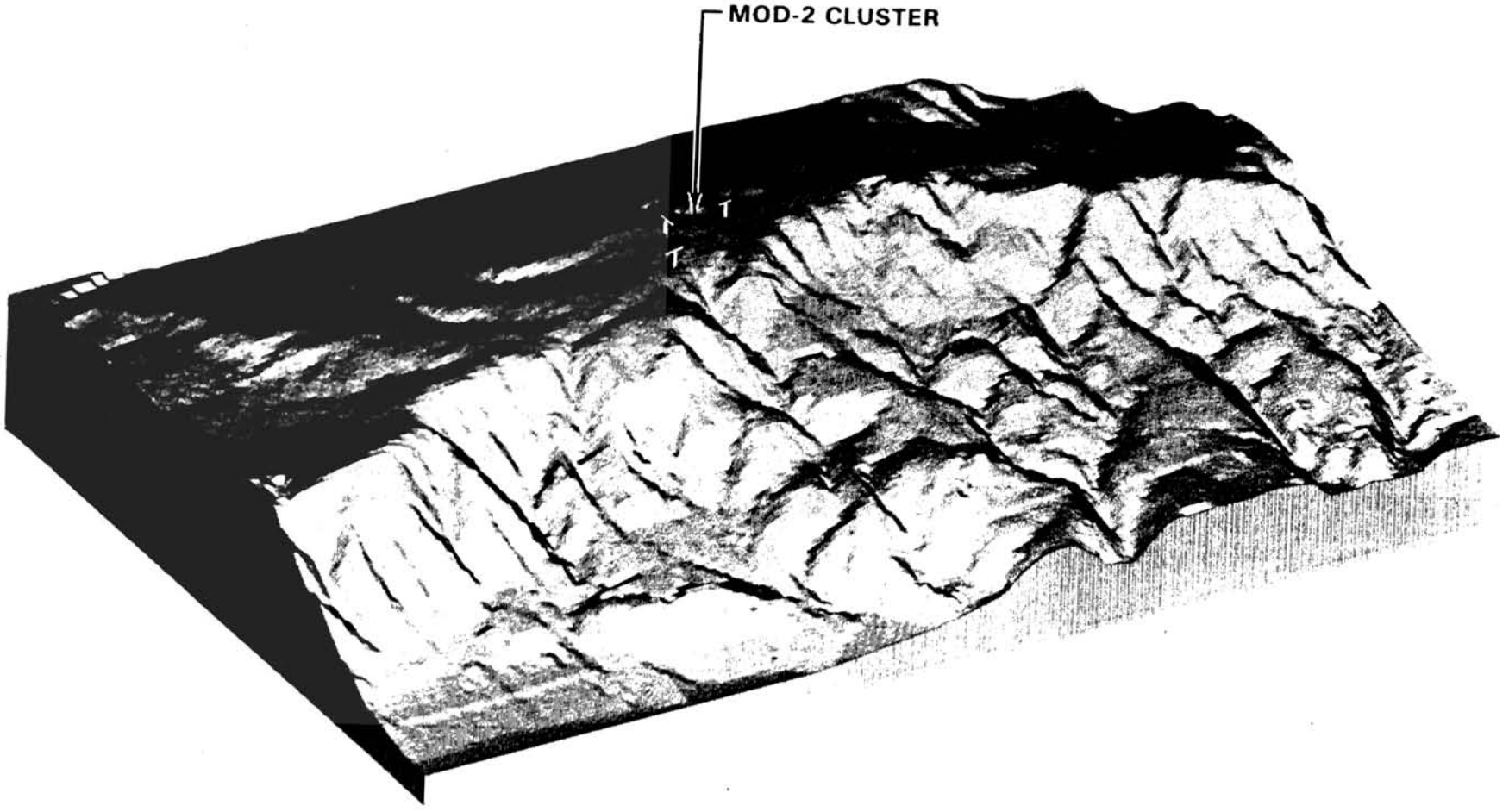

FIGURE 1.1. Computer-Enhanced Digitized Terrain Map of Site. Base dimensions are 4 by 5-1/2 miles.

Immediately following the selection of the site, a multi-agency test board was created to design and manage the experimental phase of the MOD-2 research program. This test board consisted of representatives from NASA/Lewis, BPA, BAC, Pacific Northwest Laboratory (PNL), and the Solar Energy Research Institute (SERI).

The initial actions of this test board were to establish the precise configuration of the cluster at the site and to design a data system that would support the MOD-2 research program. A triangular array was determined to be the most suitable configuration, since it would provide the best opportunity to measure the effect of the wake of an upwind machine on the performance of a downwind machine; this information is considered to be critical for future commercial wind farm activities and is a key objective of the MOD-2 test program. This triangular array would provide opportunities of monitoring wake effects at spacings of approximately 5, 7 and 10 rotor diameters (D). The data system chosen by the test board consists of a central data logging facility that monitors signals from a variety of parameters at the three wind turbines. Simultaneously, this system monitors wind speed and direction information and other meteorological parameters from two meteorological towers installed at the site: a 200-ft tower operated by the BPA and a 350-ft tower operated by PNL.

1.2 PURPOSE AND SCOPE OF THIS REPORT

The purpose of this report is to summarize the information that has been collected at the Goodnoe Hills site on machine/machine and machine/tower wake interactions. The criterion for monitoring the effect of the wake on a machine due to an upwind machine is the power deficit of the downwind machine. The criterion for monitoring the effect of a wake on a meteorological tower downwind of an operating turbine is the velocity deficit referenced to the other, "free-stream" tower. This information is an extension of preliminary results reported by Hadley and Renne (1983) and Miller, Wegley and Buck (1984). Earlier studies of wake measurements downwind of individual turbines within the Goodnoe Hills array (Liu et al. 1983; Lissaman, Gyatt and Zalay 1982; and Baker and Walker 1982) are discussed in this report in the context of the results from this analysis. The focus is primarily on momentum deficits induced by the

machine, although the turbulent characteristics of the wake are also considered to be important. Other phenomena that can affect the results of wake measurements on downwind machines, such as flow variability across the site and differences in machine operating conditions, are discussed, but are not given quantitative treatment.

The ultimate goal of this aspect of the Goodnoe Hills test program is to obtain information on potential power losses that an array of wind machines comparable to the MOD-2 could experience as a result of wakes created by upwind machines. In addition, through the more complete understanding of wake characteristics, spacing guidelines for machines of this type should evolve to maximize array performance on a given parcel of land. Although the measurements that make up the substance of this report cannot by themselves be extrapolated to fulfill these goals, this report attempts to focus on how these and additional measurements could begin to provide meaningful spacing guidelines and array performance criteria.

1.3 RELATIONSHIP TO OTHER STUDIES

Extensive information has been gathered on the structure of individual wakes using wind tunnels, numerical models, and full-scale single machine installations. Much of this information is discussed in a review by Riley et al. (1980). More recently, full-scale studies using arrays of anemometers have been conducted at the MOD-0A 200-kW test machine installed near Clayton, New Mexico (Doran and Packard 1982; Connell and George 1982). As mentioned above, extensive studies using a variety of measurement techniques were conducted on the wake of individual machines within the Goodnoe Hills cluster during the summer of 1982. However, studies of the multiple effects of wakes within arrays of wind turbines, where the turbines themselves are the "sensors" of the wake, have been limited to wind tunnels and numerical models. The Goodnoe Hills array provides the first opportunity to conduct extensive studies of machine/machine interactions from full-scale systems in a real environment. The instrumentation at the site allows a number of important parameters to be monitored simultaneously so that incident wind conditions at the site are well documented.

Although the Goodnoe Hills array has been fully operational since 1981, the data presented in this study span a three-month period during late summer and fall of 1982. During this time, all three machines were operating in a near-unattended configuration. It is from this period of time that the most comprehensive data set for exploring machine interactions with wakes is available.

2.0 REVIEW OF WAKE CHARACTERISTICS

2.1 AXIAL MOMENTUM THEORY

As a wind turbine rotor extracts energy from the wind, the downstream airflow characteristics are modified. The mean kinetic energy of the airflow is reduced, and the turbulent kinetic energy is increased. Examination of the axial momentum theory, which relates upstream and downstream velocities to turbine performance, can provide insight into the formation of the wake immediately downstream of the rotor. The process by which this occurs can be viewed conceptually from the control volume shown in Figure 2.1. For our initial treatment, the following assumptions apply (see Wilson, Lissaman and Walker 1976).

1. There is no frictional drag across the blades.
2. A well-defined stream tube separates flow through the disk from that outside the disk.
3. The static pressures far ahead and behind the rotor are equal to the free-stream static pressure.
4. Thrust loading is uniform over the rotor disk.
5. No rotation is imparted to the flow by the disk.

As the air stream passes through the actual area where it comes in contact with the rotor disk, the total head decreases. The total head decrease is due to a combination of changes in the pressure, p, and the dynamic pressure, $1/2\rho U^2$, where ρ is the density of the air and U is the mean wind speed through the rotor. For a horizontal-axis machine the change in total head is distributed uniformly across the rotor disk. The distribution of total head drop is known as disk loading. Most of the change in energy flux associated with the decrease in head represents a conversion from horizontal kinetic energy in the air to shaft torque; the remainder shows up as turbulent kinetic energy in the stream field. By applying the momentum theory to the control volume of Figure 2.1, the thrust, T, on the rotor can be written:

$$T = \text{momentum flux in} - \text{momentum flux out} \qquad (2.1)$$

or

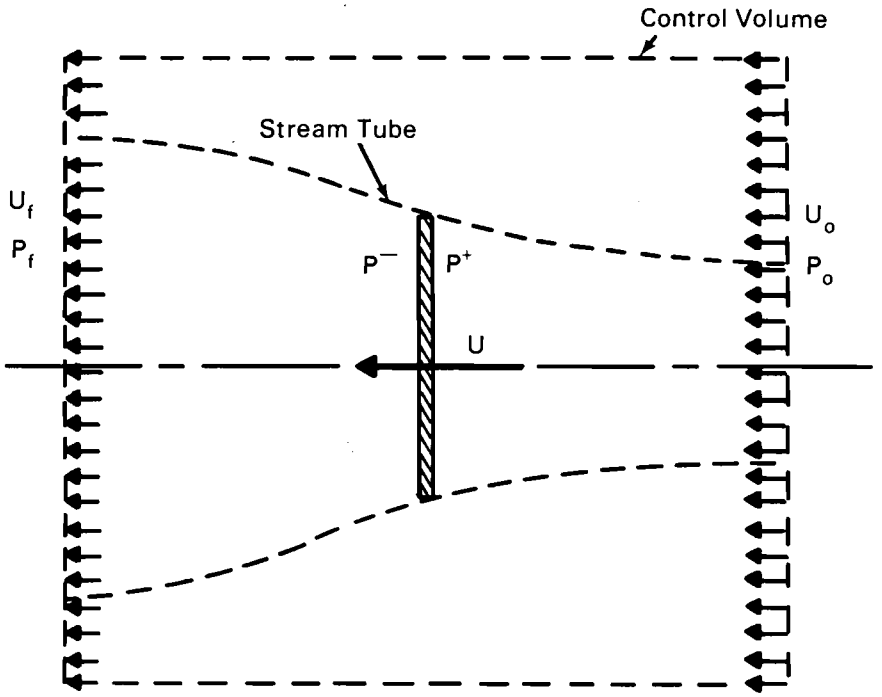

FIGURE 2.1. Schematic of the Control Volume of a Wind Turbine (from Wilson, Lissaman and Walker 1976)

$$T = \rho AU(u_o - u_f) \tag{2.2}$$

where A is the cross-sectional area of the rotor, u_o is the freestream velocity, and u_f is the wake velocity (in this case, the velocity of the wake induced directly by the rotor before any mixing of ambient air).

From pressure considerations, the thrust can also be written:

$$T = A(p^+ - p^-) \tag{2.3}$$

where p^+ is the upstream static pressure and p^- is the downstream static pressure. By applying Bernoulli's equation to both the upstream and downstream sides of the turbine and substituting into Equations (2.2) and (2.3), Wilson, Lissaman and Walker (1976) show that the thrust is given as

$$T = 1/2\ \rho A(u_o^2 - u_f^2) \tag{2.4}$$

from which we find

$$U = 1/2(u_o + u_f) \tag{2.5}$$

which states that the velocity through the rotor plane is the average of the upstream and near-wake velocities. By defining an axial induction factor, a:

$$a = 1 - U/u_o \tag{2.6}$$

we see from Equation (2.5) that

$$u_f = u_o(1 - 2a) \tag{2.7}$$

which states that the change in the final wake velocity is twice that in the rotor plane.

From Equation (2.4) it follows that the power absorbed by the rotor, P, is defined as

$$P = 1/2\rho UA(u_o^2 - u_f^2) \quad . \tag{2.8}$$

Then, from the definition of the rotor power coefficient, C_p:

$$C_p = \frac{P}{1/2\rho A u_o^3} \tag{2.9}$$

it can be shown by substituting Equations (2.5) and (2.8) into (2.9) that

$$C_{p(ideal)} = 16/27 \tag{2.10}$$

which is the theoretical Betz limit for maximum rotor power extraction efficiency. Under these ideal conditions, Wilson, Lissaman and Walker (1976) and de Vries (1979) show that the minimum velocity ratio in the wake (i.e., the maximum deficit) is

$$u_f/u_o = 1/3 \quad . \tag{2.11}$$

From the same momentum considerations that led to Equation (2.4), a thrust coefficient can be defined:

$$C_T = \frac{T}{1/2\rho A u_o^2} \quad . \tag{2.12}$$

By substituting Equation (2.4) we find

$$C_T = 1 - (u_f/u_o)^2 \quad . \tag{2.13}$$

Thus the axial momentum theory leads to an ideal thrust coefficient of

$$C_{T(ideal)} = 8/9 \quad . \tag{2.14}$$

Equations (2.10) and (2.14) can be interpreted as follows (see de Vries 1979): the power output reduction that leads to a maximum possible $C_p = 16/27$ results from the mass flow reduction through the rotor, which is a factor of 2/3. A small contribution to the power output reduction is made by incomplete energy absorption of the rotor ($C_T = 8/9$). When the rotor absorbs all the energy, i.e., $C_T = 1.0$, $a = 0.5$ and the wake velocity is zero. The power absorption of the rotor is beyond its optimum value ($C_p = 0.5$). For negative wake velocities, the axial momentum theory no longer holds for one-dimensional flow, since mass continuity is violated.

In reality, a horizontal-axis wind turbine rotor imparts rotational flow to the wake. Under these conditions, Wilson, Lissaman and Walker (1976) show that the ideal C_p is somewhat less than the Betz limit, and as a result the minimum velocity ratio is somewhat higher.

The actual C_p of a wind turbine rotor is a function of several parameters, including its "solidity" (i.e., the cross-sectional area of the rotor divided by the swept area of the rotor) and the tip speed ratio (i.e., the tip speed divided by the incoming wind speed). For a two-bladed horizontal-axis wind turbine, the maximum C_p occurs for tip speed ratios around 6.0 (Wilson and Lissaman 1974), with a maximum value considerably lower than the maximum ideal

C_p. As a result, we would expect the wake velocity to be somewhat higher than the "ideal" value of 1/3, even at the maximum rotor efficiency, and the thrust coefficient to be considerably less than 1.0. In actual practice, a wind turbine rotor is often designed to "spill" air into the wake above a certain wind velocity, so that no further power is extracted from the air as winds increase. This could occur even before the rotor reaches its maximum possible C_p; the result is that the actual maximum C_p, and therefore the maximum velocity deficit in the wake, would occur at even lower tip speed ratios.

2.2 NEAR- AND FAR-WAKE CHARACTERISTICS

The previous section has shown that, under ideal conditions, the wake velocity is a direct function of the turbine thrust coefficient, C_T. In the real atmosphere, however, turbulence is imparted to the near-wake flow through the development of rotor tip vorticies, structural shed vorticies, the formation of velocity shear zones, and mixing of ambient turbulence into the wake. The effect of this turbulence is that the wake diameter spreads and the velocity deficits decrease because of the mixing of higher ambient velocity into the wake. As a result, the near-wake conditions established by the rotor thrust can only exist for short distances downstream of the rotor. At larger and larger distances, turbulent mixing has an increasing effect on the structure of the wake.

A large variety of studies, including wind tunnel simulations, theoretical numerical modeling, and measurement programs around full-scale turbines, have been conducted to examine the characteristics of wind turbine wakes. An excellent review of these studies has been conducted by Riley et al. (1980). The measurement studies have tended to focus on characterizing the cross-wind velocity deficit profile of the wake at various downstream distances as a function of ambient turbulence intensity and some measure of machine performance, such as tip speed ratio. Generally, near-wake conditions are only observed immediately downstream of the turbine (i.e., less than four rotor diameters distant), at least for relatively nonturbulent ambient conditions. Alfreddson, Dahlberg and Bark (1980) experimented with several ambient turbulence levels in their wind tunnel tests of wake characteristics of horizontal-axis wind turbines.

They found that the near-wake region tended to vanish as the ambient turbulence increased, although the slope of the far-wake deficit profile remained essentially the same for all turbulence levels.

Vermeulen (1978) has compared momentum deficits downstream of both horizontal- and vertical-axis machines in wind tunnels. His results are shown in Figure 2.2. The transition zone between the near and far wake is clearly evident. Figure 2.3 shows results of wind tunnel tests of downstream momentum deficits for various tip speed ratios of a two-bladed horizontal-axis wind turbine, obtained from Vermuelen (1978). The slope of the momentum deficit profile in the far-wake region is about -1.25. Tennekes and Lumley (1972) have established a theoretical value of -2/3 for this slope, and it is expected that as one moves farther into the far wake this theoretical value would be approached in Vermeulen's analysis.

Turbulence intensity values have also been studied in wind tunnel experiments. Figure 2.3 shows profiles of turbulence intensities for the three different tip speed ratios of the two-bladed horizontal-axis machine, obtained from Vermeulen (1978). A high turbulence intensity level is observed in the transition zone between the near- and far-wake regions, associated with turbulence generated by the shear layer. Turbulence intensities appear to be higher in the wake than in ambient air, and appear to be a function of tip speed ratio. These higher values result in part from the lower mean wind speeds used to calculate turbulence intensity.

These studies (as well as others too numerous to document here) confirm the general pattern of a wake structure downwind of the turbine. The strength of the near wake is primarily a function of rotor thrust, which can be related to tip speed ratio. Only under very high ambient turbulence conditions does the near-wake structure vanish. The near wake shows a constant velocity deficit value at the centerline out to as much as four rotor diameters from the rotor plane. The wake then exhibits a transition from near-wake to far-wake conditions, where in the far wake a gradually decreasing momentum deficit is observed. The distance of this transition zone is often a function of ambient turbulence intensity (and, to a lesser extent, rotor-induced turbulence); however, the slope of the downwind momentum deficit profile is often the same

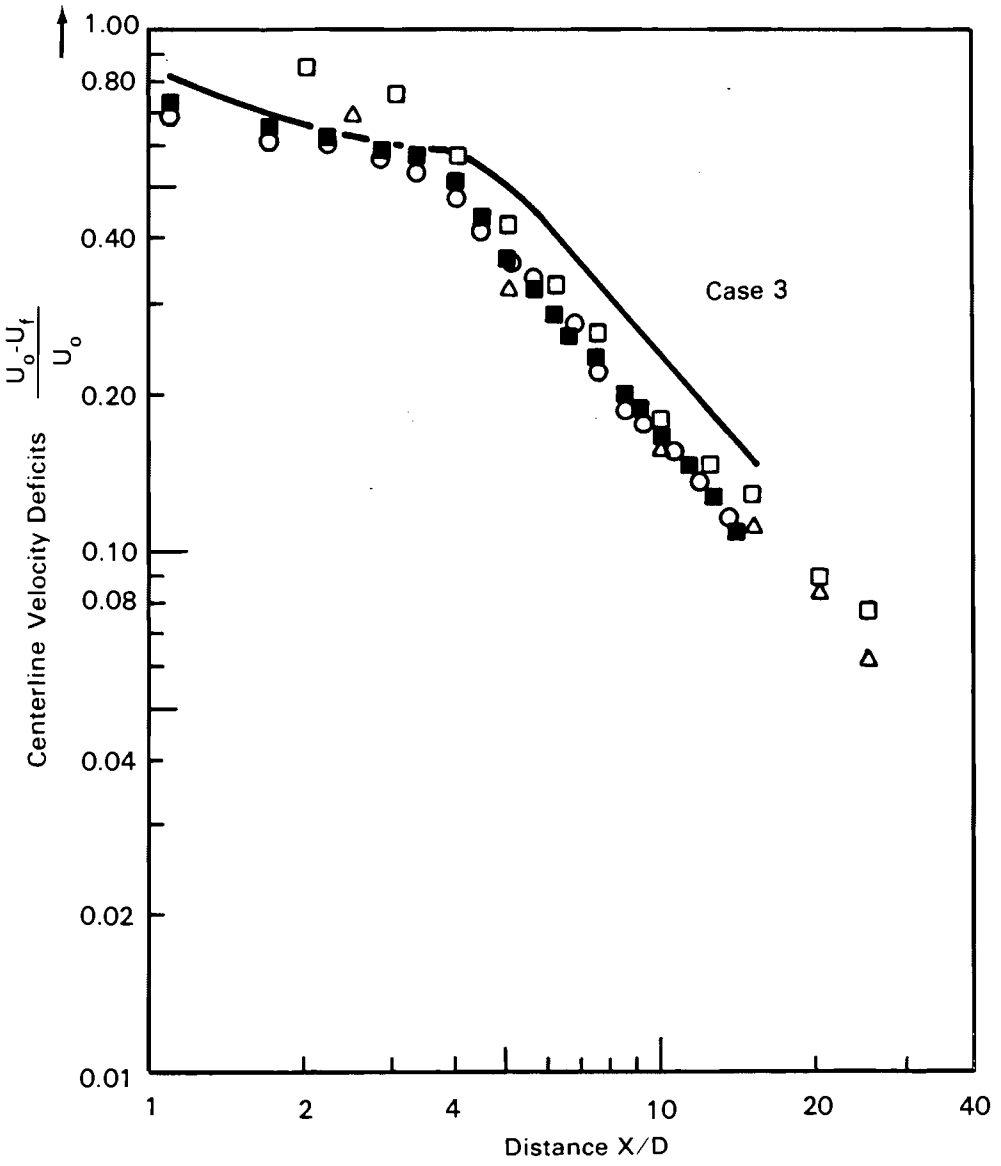

Flow Case No.:

	1	2
Darrieus Turbine	□	△
Horizontal Axis Turbine	■	○

FIGURE 2.2. Comparison of Wind Tunnel Results of Momentum Deficits Downstream for Horizontal- and Vertical-Axis Turbines (from Vermeulen 1979)

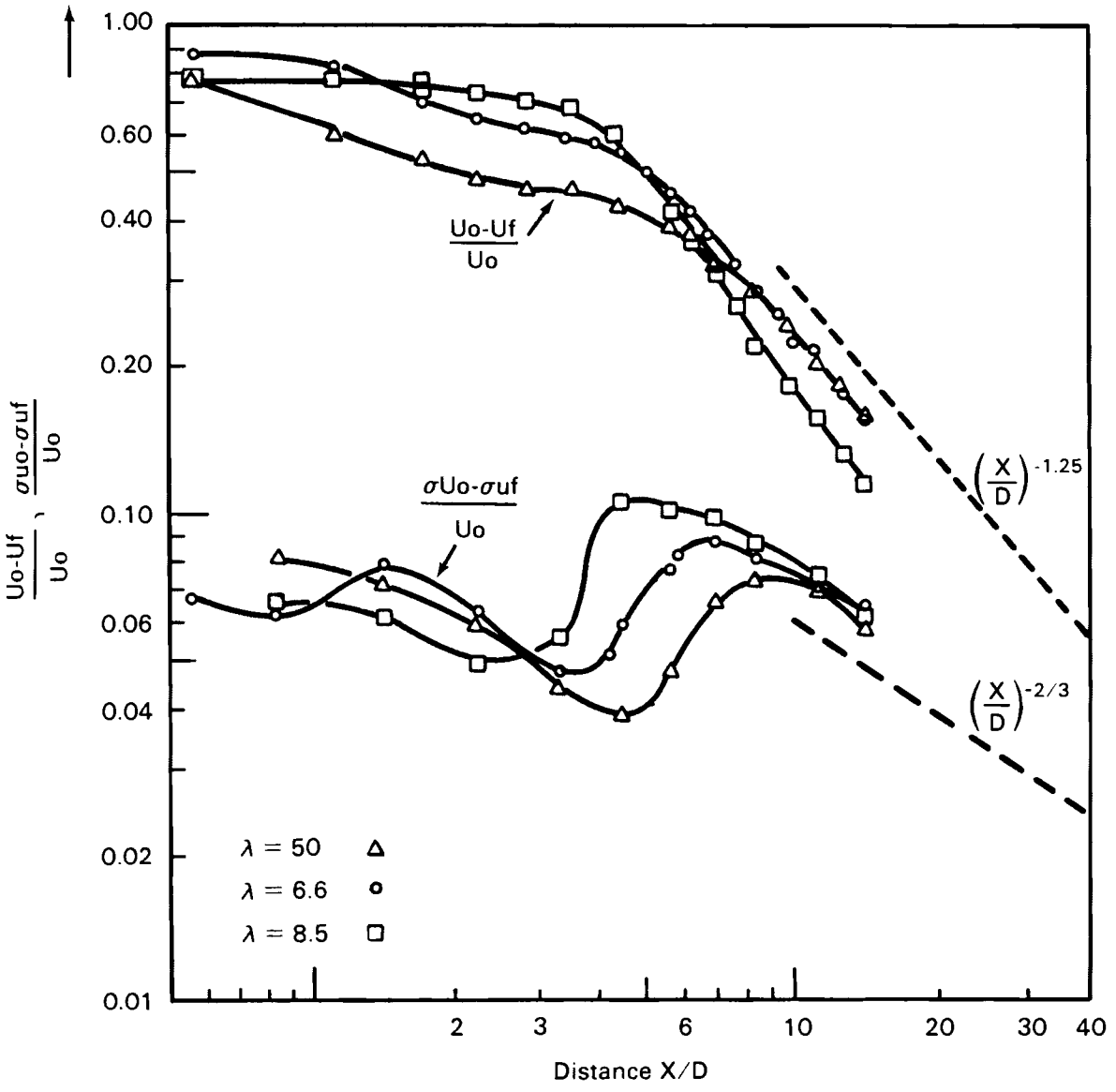

FIGURE 2.3. Wind Tunnel Results of Momentum Deficits (Top Three Curves) and Normalized Turbulence Intensities (Bottom Three Curves) for Three Tip Speed Ratios of a Two-Bladed, Horizontal-Axis Wind Turbine (from Vermeulen 1978)

regardless of the turbulence level. Thus, the far-wake structure is established almost entirely by the degree of ambient transverse turbulence in the atmosphere--the component of turbulence that actually causes wake expansion.

2.3 NUMERICAL WAKE MODELS

The most extensive numerical development of the wake phenomenon has been by Lissaman (1979) (see also Walker and Lissaman 1978; Lissaman 1977; and Lissaman and Bate 1977). This model draws upon an analogy between wind turbine wakes and jet-like flows, where in this case the wake, although moving in the same direction as ambient flow, has lower velocity than ambient. This approach is based on the work by Abramovich (1963). In Lissaman's model, the wake is divided into the near-wake core and the far-wake field. In the near wake, a uniform velocity deficit profile is assumed across the wake. The turbulence generated by the strong shear at the edge of the wake acts to expand the wake. In the far wake, the velocity profile across the wake is assumed to be nearly Gaussian. The wake continues to expand as a result of entrainment of ambient turbulence and of the internal generation of turbulence in the shear zone at the edge of the wake.

The two conditions needed to predict the downstream structure of the wake are the maximum velocity deficit in the near-wake field and the wake radius. The first condition is determined by the operating characteristics of the wind turbine, such as the power coefficient, which can be related to the thrust coefficient. The second condition is determined by the ambient turbulence intensity and the wake turbulence. Other features incorporated by Lissaman's model include the tower wake, the effect of vertical wind shear, and ground effects, which are accounted for by classical reflection techniques.

Recently, Lissaman, Gyatt and Zalay (1982) modified the model to provide a turbulent growth algorithm that fits experimental data. Other modifications include the incorporation of viscous drag on the rotor, the effect of pressure variations in the wake, a more precise algorithm for depicting the wake radius at the end of the potential core region, and the effect of the wind speed profile in the planetary boundary layer on wind turbine performance. The effect of these modifications is that the current version shows more rapid wake decay

than the original version. The results are more consistent with wind tunnel observations.

Other models similar to the Lissaman version have also been developed, such as that by Eberle (1981). Ainslie (1982) recently compared three models, all of which have similar philosophy and computational structure: the Lissaman model, the TNO (The Netherlands Organization for Industrial Research) model called "Milly" (Vermeulen and Builtjes 1981), and the CERL (Central Electricity Research Lab) model called EMWAC (Ainslie 1981). Although all three models agreed reasonably well with wind tunnel data, large differences did occur and none of the models gave consistently good agreement.

Entirely different approaches have been attempted by Sforza et al. (1979), Crafoord (1979), and Ainslie (1983). These models begin from basic boundary-layer principles. Although these techniques allow a more detailed and thorough examination of the important parameters governing the structure and behavior a wind turbine wake, their complexity makes them unsuitable for modeling wakes associated with arrays of wind turbines.

A more simplified approach has been taken by Baker and Walker (1982) following a series of field measurements of wake characteristics at Goodnoe Hills. The basis of this model is the axial momentum theory described in the first section of this chapter. Empirical relationships of rotor thrust and transverse turbulence are developed from the data collected at Goodnoe Hills, so that the centerline velocity deficit equation reduces to a simple equation that is a function of these two parameters only.

The modified Lissaman (1982) and simplified wake (Baker and Walker 1982) models will be compared against the observations of wake deficits obtained from the machines and fixed towers at Goodnoe Hills evaluated in this report. These comparisons are presented in Chapter 5.0.

3.0 GOODNOE HILLS DATA COLLECTION PROGRAM

3.1 SOURCES OF DATA AT THE MOD-2 TEST SITE

Various sensors have been installed for routine measurements at the three MOD-2 wind turbine systems and two meteorological towers installed at the Goodnoe Hills array. At the time of this study, each turbine had sensors recording the wind speed measured from the nacelle anemometers, the generator field current and power output, the "utility power" (the actual power going into the BPA system), the generator voltage, rotor speed, blade pitch angle, and the relative position of the nacelle. The 350-ft meteorological tower operated by PNL had wind speed and direction sensors at the 33-, 50-, 200-, and 350-ft levels, temperature sensors at the 33- and 350-ft levels, and an atmospheric pressure sensor at the 200-ft level. The 200-ft tower operated by BPA had wind speed and direction sensors at the 50- and 195-ft levels, a temperature sensor at the 50-ft level, and an atmospheric pressure sensor at the base of the tower. This tower was also equipped with a sensor to detect the buildup of ice.

During certain periods, other sensors were installed on the towers to obtain special measurements for specific studies. For example, during the summer of 1982, when wake studies were under way, uvw anemometers were installed at the 200-ft level at both towers. These sensors remained on the towers after the summer studies and were available during the period of time that machine/machine and machine/tower wake interaction data were collected (see Section 3.2).

3.2 GOODNOE HILLS DISTRIBUTED DATA SYSTEM

A centralized data logging system, known as the Distributed Data System (DDS), was installed at the site to monitor data collected from both of the meteorological towers and from the three wind turbines. The DDS consists of a microcomputer hard-surface disk drive, a terminal, and a tape drive for backup storage. The disk is used as a load device for the computer software and as storage for the collected data.

The DDS is designed to collect and record data parameters on a common time basis transmitted from different locations around the site. The data are

transmitted through a fiber optics cable system that is buried underground and runs from the three turbines and two towers to a centralized location. The fiber optics are connected to the microcomputer. Figure 3.1 provides a schematic of the various components of the DDS at the site.

The time reference is controlled by a battery-operated clock that will not lose time even if there is an electrical power failure. If power to the data room is shut off, the computer will close the current data file to prevent data loss. When the power is off no data are collected. Once the power is back on, the DDS will automatically restart the computer and give it the current time from the clock. The DDS will begin a new data file with the current time.

The software provided with the DDS gives the user the following data collection options:

- selection of data channels to be contained by the data file
- selection of data sampling interval
- selection of data sampling format (averaged or instantaneous values with standard deviations)
- selection of the time period of the data file.

Once these options are decided, the system can be programmed to collect exactly the data the user wants. In normal operations, the DDS at the Goodnoe Hills Site collects 50 channels of data: 16 channels from the PNL tower, 10 channels from the BPA tower, and 8 channels each from turbines #1, #2, and #3. The sample rate is one per second and the data are averaged every 2 minutes. A standard deviation is also computed for every parameter collected. The time period for the data files is 1 day.

Other software in the computer provides monitoring functions, such as which data files are active and which channels are being collected in the file. Other monitoring functions, such as the number of data files already created, and the amount of free space available on the disk, are also on the system. This software improves the reliability with which the data can be collected.

The DDS became operational on August 16, 1981. At that time, only the data from the two meteorological towers were being recorded on the system.

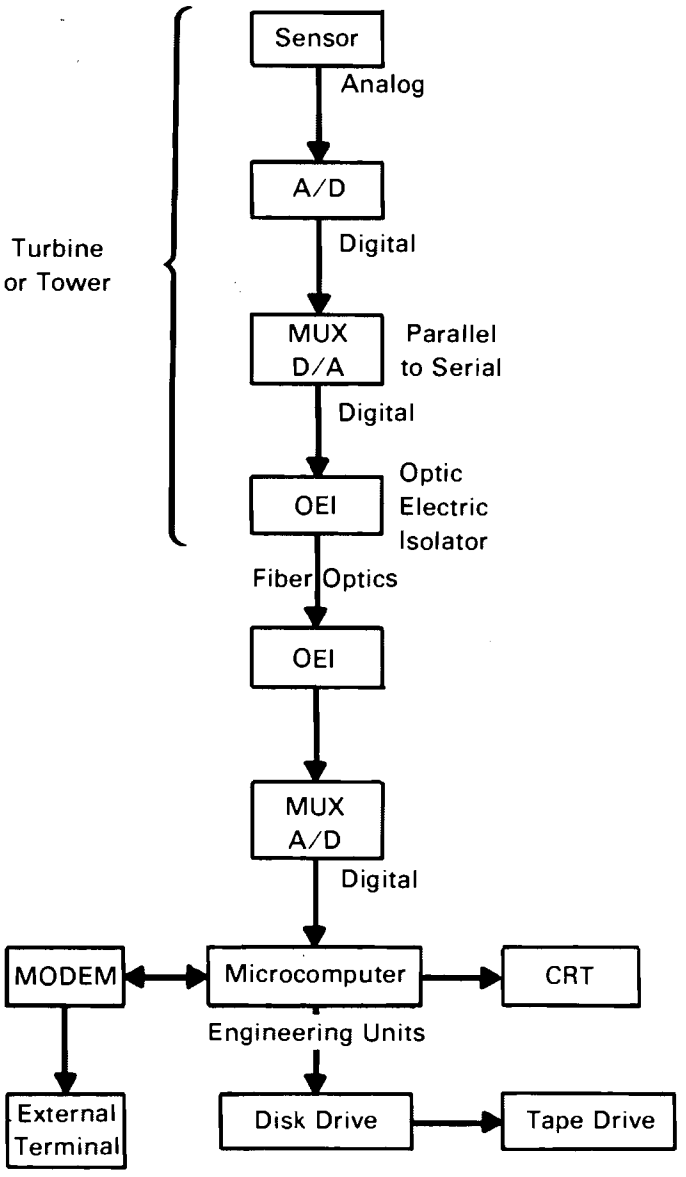

FIGURE 3.1. Schematic of the Information Flow Through the Distributed Data System (DDS) at the Goodnoe Hills Site

Data from turbine #1 were incorporated into the system in the spring of 1982. However, shortly after that time the DDS suffered a failure and was not made operational until later that summer, when data from the towers were once again recorded by the system. On August 29, 1982, turbines #1 and #3 were connected to the DDS and later, on October 6, turbine #2 was connected. On November 12, all machine operations at the site were stopped when a crack was discovered in the low-speed shaft of turbine #1. As a result, the data set from the period August 29 to November 12, 1982, formed the basis for the analysis of machine/machine and machine/tower wake interactions presented in this report. Table 3.1 lists the parameters that were collected by the DDS during this period.

3.3 DEFINITION OF DATA SETS USED FOR WAKES ANALYSES

The channels chosen for analysis of machine/machine and machine/tower wake interactions during the August 29 to November 12, 1982, data period are shown in Table 3.2. As stated above, data from each channel consisted of a 2-min average and a standard deviation of the 1-s values. From October 21 through October 31 the averaging period was changed to 5 s. These 5-s data were averaged to create 2-min samples that would correspond to the remainder of the data set.

Once the data set was constructed, the calibrations were checked using the MOD-2 operation log books provided by BAC. For machine/machine wake interactions, the data were edited so that only those periods when the PNL 200-ft wind speed was greater than 13.0 mph were saved. The periods when the winds were less then 13.0 mph were not incorporated into the data since the turbine cut-in speed is 14.0 mph.

The data set was modified somewhat for examining machine/tower wake interactions. For these specific cases, the wind speed restrictions were lifted. Had this not been the case, much of the data when the PNL tower was in the wake of a turbine would have been eliminated, since the wake wind velocity was often below the 13 mph value established for examining machine/machine wake interactions.

TABLE 3.1. Data Channels Collected on DDS During Period August 29 to November 12, 1982

PNL tower:

1) wind direction at 33 ft
2) wind direction at 50 ft
3) wind direction at 200 ft
4) wind direction at 350 ft
5) wind speed at 33 ft
6) wind speed at 50 ft
7) wind speed at 200 ft
8) wind speed at 350 ft
9) temperature at 33 ft
10) temperature difference between 350 ft and 33 ft
11) air flow at 33 ft
12) air flow at 350 ft
13) pressure at 200 ft
14) u-component at 200 ft
15) v-component at 200 ft
16) w-component at 200 ft

BPA tower:

1) wind speed at 50 ft
2) wind direction at 50 ft
3) wind speed at 195 ft
4) wind direction at 195 ft
5) temperature at 50 ft
6) pressure at ground level
7) ice detector
8) u-component at 200 ft
9) v-component at 200 ft
10) w-component at 200 ft

Turbine #1, #2, #3:

1) field current
2) generator power
3) utility power
4) generator voltage
5) rotor speed
6) blade #1 pitch
7) yaw error
8) nacelle position

TABLE 3.2. Data Channels Chosen for Wakes Analysis During Period August 29 to November 12, 1982

1) PNL wind direction at 50 ft
2) PNL wind direction at 200 ft
3) PNL wind direction at 350 ft
4) PNL wind speed at 50 ft
5) PNL wind speed at 200 ft
6) PNL wind speed at 350 ft
7) BPA wind speed at 195 ft
8) BPA wind direction at 195 ft
9) Turbine #1 generator power
10) Turbine #1 nacelle position
11) Turbine #2 generator power
12) Turbine #2 nacelle position
13) Turbine #3 generator power
14) Turbine #3 nacelle position

The data set was also edited to include only those conditions when a turbine or a tower could be in a wake of a turbine. This was done by examining the layout of the site, as shown in Figures 3.2 and 3.3. From these figures, the wind directions necessary for the center of the wake (assuming straight-line flow) to impinge on a downwind turbine or tower for each possible case of machine/machine or machine/tower wake interactions were determined. Then, all wind directions ±30° of each of these wind directions were incorporated into the data set. Figure 3.3 provides these wind directions, as well as the downwind distance in rotor diameters, for which centerline wake data could be obtained from any machine/machine or machine/tower interaction.

The programs used to analyze this data set were structured to ensure that the rotor speed was at least 17 rpm and that the generator power was greater than 50.0 kW. Any data below these values were not used for wake analyses. The data from the two towers were also edited for possible erroneous values. A comparison of the tower data at the 50-ft levels indicates a good correlation between towers both in wind speed and direction. The exception to this was when the winds originated from 45° to 120°. Under these conditions, the meteorological tower structure itself "shadows" the wind sensors, leading to a lower-than-actual measured wind speed. However, for the most part the winds that represent the best energy potential are from 180° to 360°. This had been foreseen before the turbines and towers were positioned, so that no significant loss of data results when winds are out of the northeast.

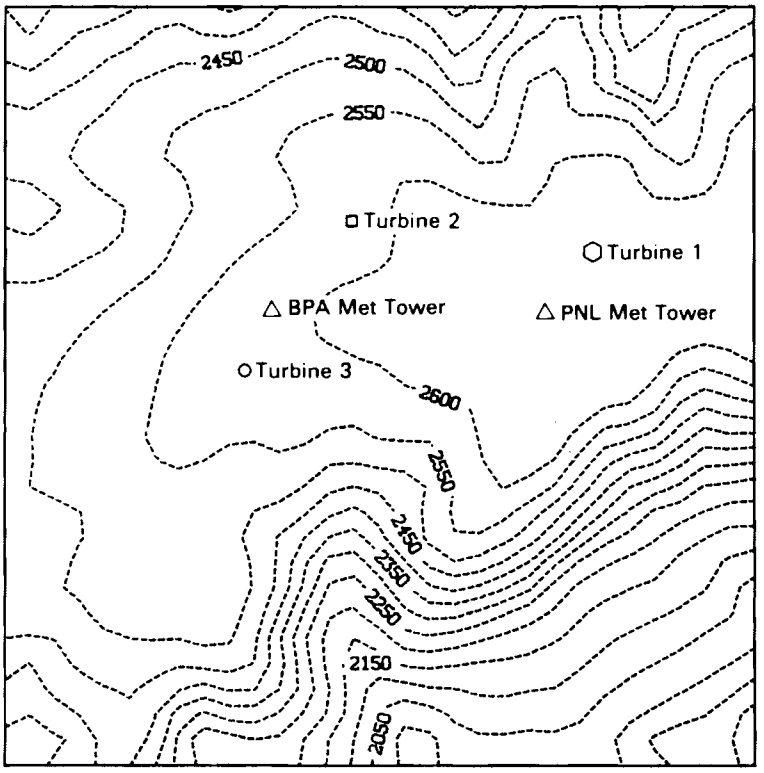

FIGURE 3.2. Relative Position of the Three MOD-2 Wind Turbine Systems and Two Meteorological Towers at the Goodnoe Hills Site

Turbine	#1	#2	#3	BPA	PNL
#1	--	6.7 D 96°	10.2 D 73°	9.0 D 82°	2.2 D 42°
#2	6.7 D 276°	--	5.0 D 40°	3.3 D 46°	5.8 D 292°
#3	10.2 D 253°	5.0 D 110°	--	1.7 D 207°	8.3 D 260°

FIGURE 3.3. Incident Wind Directions Necessary for Centerline Wake Interactions and Relative Distances for All Combinations of Turbines and Towers. The relative locations of turbines and towers are repeated for reference.

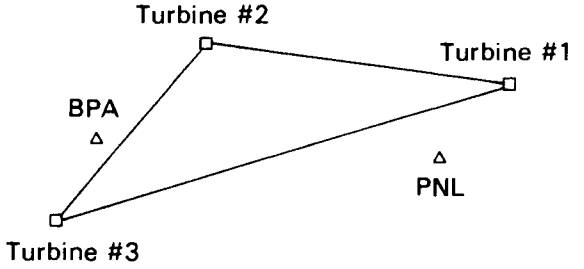

The wind speed data at the 200-ft level show a good correlation between towers, but the PNL wind directions are generally 15° to 18° higher (i.e., more northerly for westerly winds) than those measured at the BPA tower. After realignment the error disappeared. This difference has been noted before and has not been satisfactorily explained. There is a strong indication that at least part of this discrepancy is actual and is caused by the complex terrain at the site.

4.0 OBSERVATIONS OF WAKES IN THE ARRAY

4.1 BACKGROUND FLOW CHARACTERISTICS

For this study, downwind meteorological towers or wind turbines represent the "sensors" of the structure of wakes caused by an upwind machine. However, before the wake characteristics can be evaluated, it is first necessary to determine if background flow characteristics or sensor calibration errors exist that could mask an actual wake measurement. To do this, one year of data was analyzed at each of the meteorological towers for a period beginning September 1, 1981. Hourly concurrent wind speeds at the 200-ft level of the PNL tower were divided by those at the 195-ft level of the BPA tower and averaged in 5° direction bins based on the 200-ft PNL wind direction sensor. The results of this analysis are shown in Figure 4.1.

Significant differences in average wind speed are noted for two background wind direction ranges. As shown in Figure 4.1, for an incident wind direction around 60°, measured wind speeds at the PNL tower are significantly lower than those at the BPA tower, while the opposite occurs for incident wind directions around 100°. The cause of these differences is the effect of the meteorological tower structure on the sensors themselves. Since the prevailing winds at the site are westerly, the booms supporting the anemometers were oriented toward the west when mounted on the towers. As a result, the anemometers are in the wake of the tower when winds are out of the east. The booms on the PNL tower are oriented toward the southwest, while those on the BPA tower are oriented directly toward the west. As a result, the tower shadow occurs for wind directions from 60° to 90° at the PNL tower and from 100° to 130° at the BPA tower.

Figure 4.1 shows that even for westerly winds some differences exist between wind speeds measured at the two towers. Winds blowing from the predominant power-producing directions, 220° to 300°, tend to be higher at the BPA tower, particularly for southwesterly flow. In the wind direction range 240° to 300°, the BPA 195-ft wind speeds average about 3% higher than those at the PNL 200-ft level.

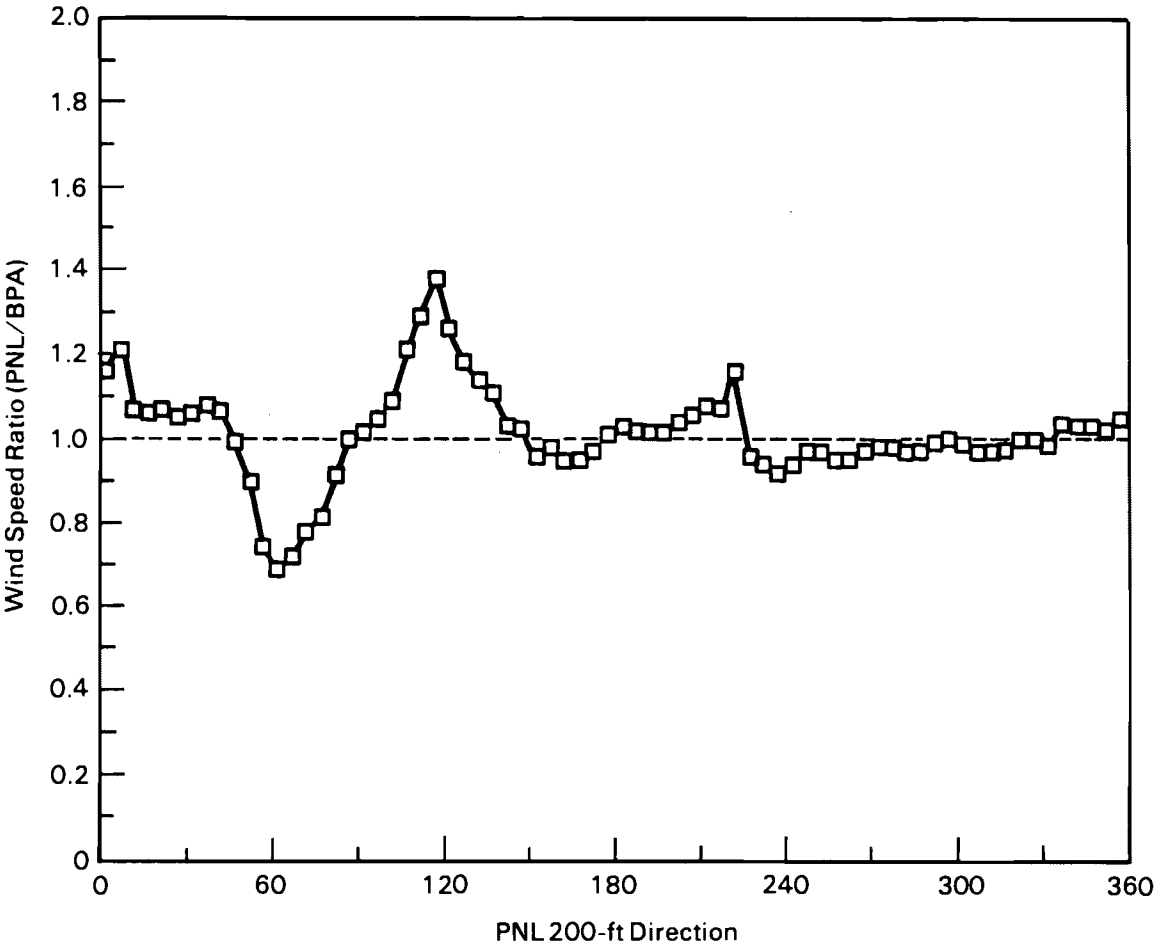

FIGURE 4.1. Wind Speed Ratio Averaged by 5° Bins (200 ft PNL/195 Ft BPA as a Function of PNL 200-ft Wind Direction Based on 2-min Averaged Data from 9/01/82 to 8/31/83 at Goodnoe Hills.

The velocity ratios were also calculated for different wind speed classes in the 240° to 300° wind direction range. The results (not presented here) showed that the difference between the two towers was essentially the same over all wind speeds within the operating range of the MOD-2, with the PNL tower ranging from 1% to 4% lower than BPA. Differences tended to be smaller at higher wind speeds. This difference could be terrain-induced, or could result from inherent differences in sensors between the two towers. The differences are small enough so as not to be taken into account when evaluating wake characteristics at the towers (Section 4.5).

4.2 COMPARISON OF MOD-2 POWER CURVES

To determine if differences in power output between the turbines at any given time corresponded to differences in wind speeds at those locations, power curves for turbines #1 and #3 were calculated. If the power curves for the two machines were identical when evaluated against the wind speed from the same meteorological tower, this would indicate that both machines have identical operating characteristics. The power curves for turbines #1 and #3 were calculated using the 200-ft level wind speed at the PNL tower. The calculations were based on all wind directions when turbine wakes would not interfere. The results are shown in Figure 4.2.

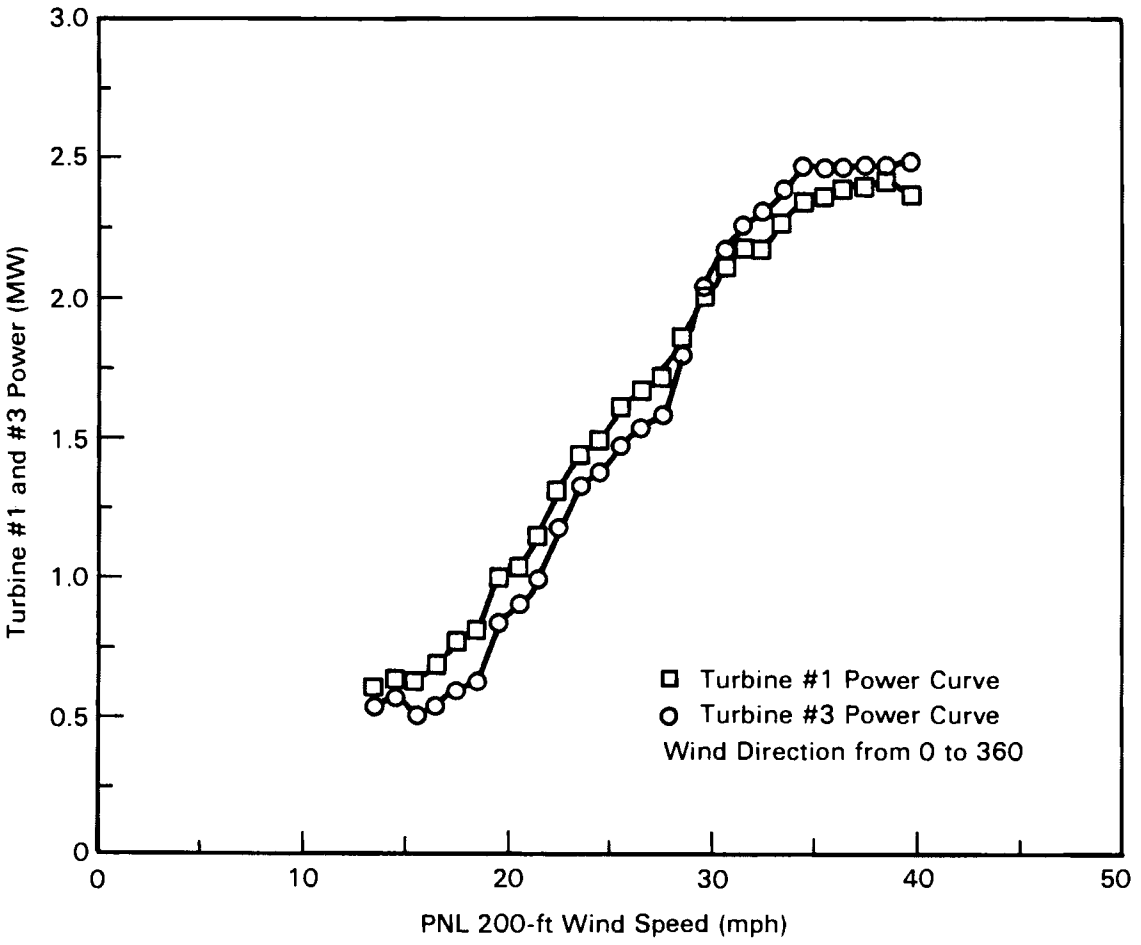

FIGURE 4.2. Power Curves for Turbines #1 and #3 Calculated Using the 200-ft-Level Wind Speed at PNL Tower Based on Data from All Wind Directions.

Figure 4.2 shows that the power curves for the two machines are quite similar. For wind speeds less than 30 mph, turbine #1 produces approximately 10% more power than turbine #3 at any given speed. Since most of the power-producing winds at the site are less than 30 mph, one might expect turbine #1 values to be higher than turbine #3 values for a given wind speed, even though winds tend to measure slightly lower at the PNL tower, which is near turbine #1. However, since these analyses represent averages of large amounts of data with a fair amount of scatter, no attempt is made to rectify discrepancies in results of turbine power output comparisons and tower wind speed comparisons for the wake analyses.

A power curve for turbine #2 was also calculated. However, since this turbine had much less run time than the other two during the August 29 to November 12, 1982, period, the resulting power curve was inadequate from which to draw comparisons with the other two turbines.

4.3 OBSERVATIONAL EVIDENCE OF WAKES AT GOODNOE HILLS

The August 29 to November 12 data set was first screened to determine if any evidence of wakes on downwind turbines appears statistically. The results of this survey are displayed using contingency tables, shown in Tables 4.1, 4.2, and 4.3. These tables present the percentage of observations when a downwind turbine shows less power output than an upwind turbine when the wind direction is aligned from the upwind to the downwind turbine. The wind directions necessary for this alignment were shown in Figure 4.3. Tables 4.1, 4.2, and 4.3 also provide the percentage of observations when the downwind turbine showed greater power than the upwind turbine for this wind direction and provide a comparison of the downwind to upwind turbine for wind directions beyond ±7.5° from that which is aligned with the turbines. From these tables, it is clear that if a significantly greater percentage of observations is shown of lower power output when the downwind turbine would be expected to be in the wake of the upwind turbine, then it can be assumed that the measurements reflect the effect of a wake on the downwind turbine. This would be particularly true if the observations of downwind turbine power were approximately 50% above and 50% below the upwind turbine when wind directions are not aligned with the two turbines.

TABLE 4.1. Number of Observations of 2-min Averages of Power Differences Between Turbines #1 and #3 (Separated by 10.2 D) for Cases When the Winds Are Aligned Along the Machines and for Other Cases

	Turbine Power Output Comparison	
	T1 ≥ T3	T1 < T3
Wind Direction = 253° ± 7.5°	123	88
	58.3%	41.9%
Other Wind Direction	945	427
	68.8%	31.2%

TABLE 4.2. Number of Observations of 2-min Averages of Power Differences Between Turbines #1 and #2 (Separated by 6.7 D) for Cases When the Winds are Aligned Along the Machines and All Other Cases

	Turbine Power Output Comparison	
	T1 ≥ T2	T1 < T2
Wind Direction = 276° ± 7.5°	40	101
	28.4%	71.6%
Other Wind Direction	106	95
	52.7%	47.3%

TABLE 4.3. Number of Observations of 2-min Averages of Power Differences Between Turbines #2 and #3 (Separated by 5.0 D) for Cases When the Winds are Aligned Along the Machines and All Other Cases

	Turbine Power Output Comparison	
	T2 ≥ T3	T2 < T3
Wind Direction = 220° ± 7.5°	0	0
	0.0%	0.0%
Other Wind Direction	40	16
	71.4%	28.6%

Table 4.1 shows that turbine #1 power is higher than turbine #3 normally and even when #1 is in the wake of #3. This would be consistent with Figure 4.2, which shows that turbine #1 in general produces more power than turbine #3. As a result, for this turbine pair this analytical scheme does not reveal any

significant wake effect on the downwind turbine, since the difference in power between the turbines masks any effects that could be shown by this technique.

For turbines #1 and #2, Table 4.2 shows that the downwind turbine (#1) produces less power most of the time when the winds are aligned along these two machines. For other wind directions, the fact that the observations show turbine #1 producing more power than turbine #2 about half the time, and less power the remaining half, indicates the two machines normally operate with essentially the same power curve. Thus, the table for these two machines indicates a substantial number of observations when the downwind machine is losing power due to the wake of the upwind machine.

For the case of turbines #2 and #3, Table 4.3 indicates that there are insufficient data to identify any wake effects. As a result, these tables only provide strong evidence of wake effects between turbines #2 and #1, which are separated by 6.7 D.

4.4 POWER RATIOS AS A FUNCTION OF INCIDENT WIND DIRECTION

In the previous sections of this report, the data analyses indicated that turbine #1 is often affected by the wake of turbine #2 when the wind direction is aligned along those two machines. It was difficult to see any evidence of wake effects between turbines #1 and #3 because of an apparent discrepancy in machine power output for a given wind measurement. Furthermore, insufficient data were available to evaluate statistically if wake effects could be discerned between turbines #2 and #3. In this section, we attempt to identify wake effects through other analytical schemes.

The data were sorted into wind direction bins 1° in width. Then, for each pair of machines, the power ratio was calculated from the average of all observations in each wind direction bin. Further, the wind directions were referenced to the orientation of the respective turbines, so that an incident direction of 0° represented a wind aligned directly with the two turbines. This was done by subtracting the direction of turbine alignment from the actual wind direction. Thus, a negative value on the scale represents winds blowing from a more southerly direction with respect to the alignment direction.

The power ratio is always defined as the ratio of the downstream machine power output to the upstream machine power output, so that a wake effect would appear as a value less than 1.0 if the machine power curves are the same.

Data are not available for specific wind conditions when turbines #2 and #3 were running; therefore, no analysis can be done for this 5.0-D case. There are available 1032 two-min data values when the winds were ±30° of the wake centerline between turbine #1 and #3 with both machines running. A total of 246 data points are available for the same criteria between turbines #1 and #2.

Turbine #1 and #3 interaction was defined as winds ±15° from the centerline of the wake between the two turbines, which was 253°. The distance between these two turbines is 10.2 D. The criteria for a turbine to be running were 1) the wind speed at the "free-stream" meteorological tower had to be >13 mph; 2) the power from both turbines had to be above 50 kW; 3) both machines had to be rotating at greater than 17 rpm; and 4) the third machine could not be running (except when all three machines were being studied).

Figure 4.3 shows the power ratio of turbine #1 to turbine #3 as a function of incident reference wind direction without any averaging. This figure shows the large amount of scatter in the data. Once the data have been averaged for each wind direction bin, a pattern appears that is seen in Figure 4.4.

A power deficit near the wake centerline can be seen in Figure 4.4. This deficit is assumed to be the result of lost power caused by the wake of turbine #3. The magnitude of this deficit is about 15%. A cubic spline fit to the data points has been included to aid the reader in identifying patterns in the data. The standard deviations of the power ratios are also plotted to give an idea of the scatter involved for each point.

The center of the wake appears to be a few degrees to the south of the centerline. This could result from instrument difference or curvature of the wind caused by the terrain at the site. The figure also indicates that the wake does not seem symmetric but, rather, is skewed toward the south. This could be an artifact of the averaging and binning of the data, or it could be a result of wind behavior at the site: the wind speeds at the site tend to be slower for more southerly directions. The surface layer is larger and,

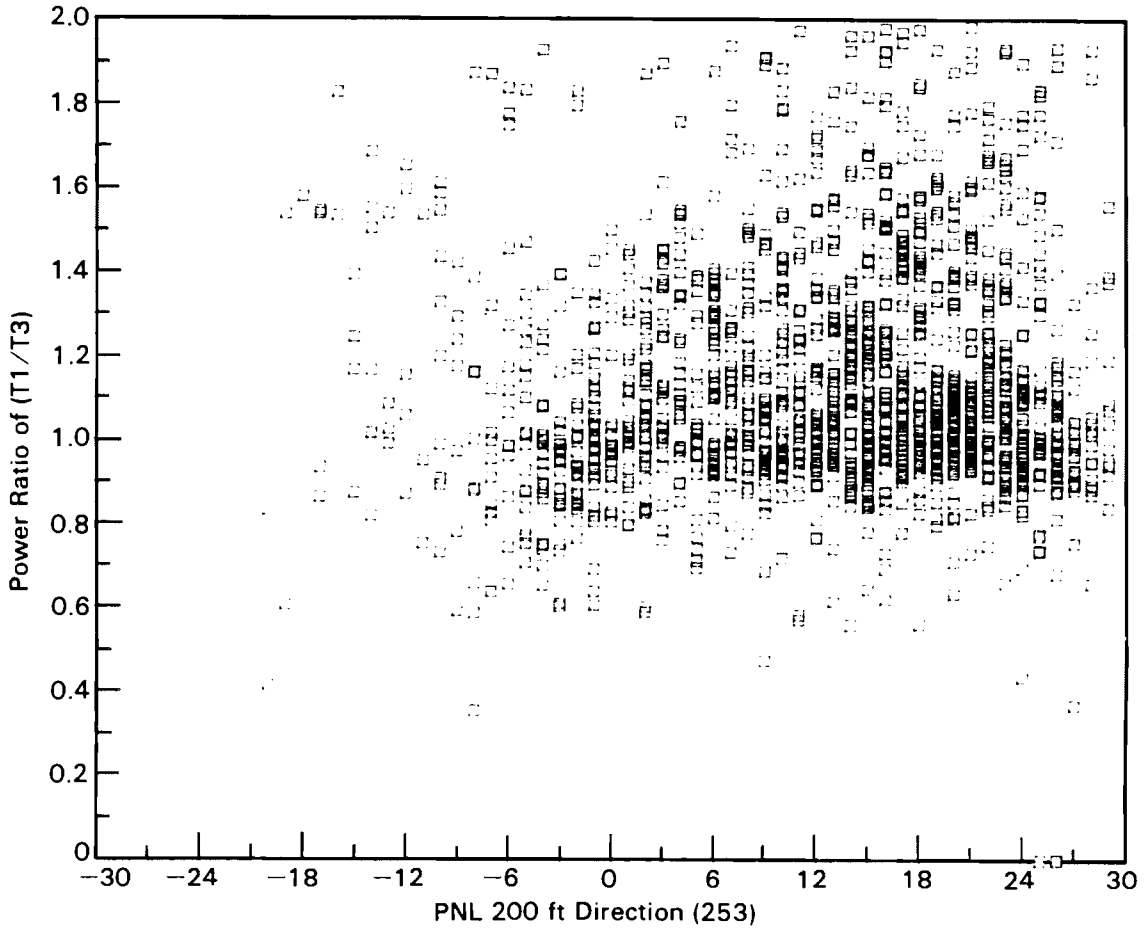

FIGURE 4.3. Power Ratio of Turbine #1 to Turbine #3 as a Function of Incident Reference Wind Direction (253°) Without Any Averaging.

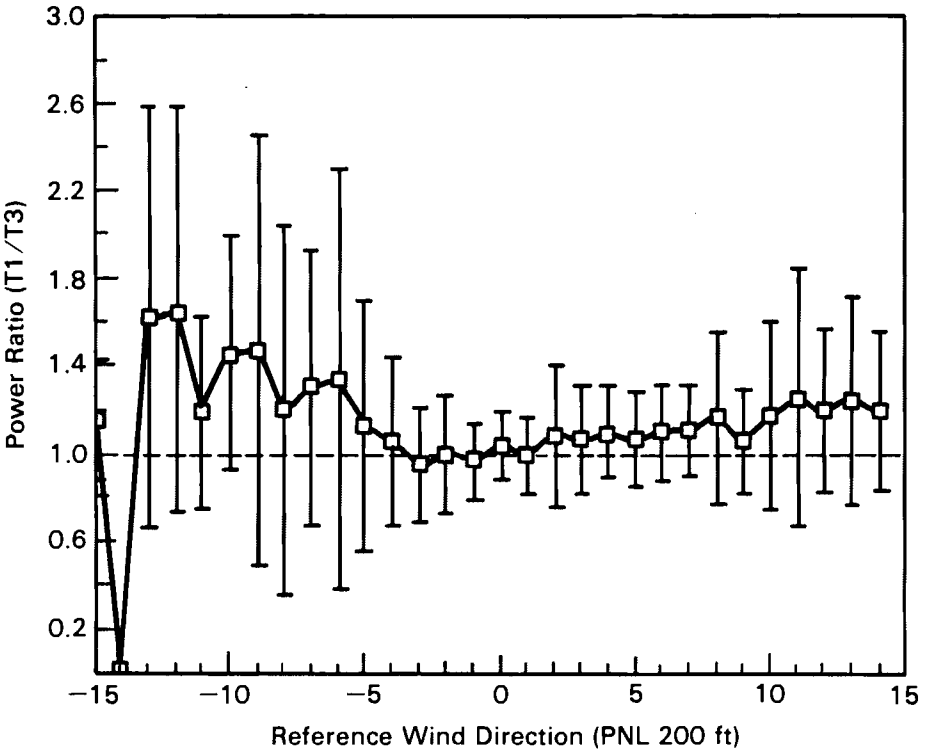

FIGURE 4.4. Power Ratio of Turbine #1 to Turbine #3 as a Function of the Incident Reference Wind Direction (233°) Averaged by 1° Bins. The standard deviations of the ratios are also plotted.

therefore, has more influence on the flow for these lighter winds, causing additional frictional veering of flow toward the south. This characteristic would result in a steeper wake profile on the southerly side of the reference wake centerline direction. Recent kite data obtained by Oregon State University also indicated a nonsymmetric wake (January 1985).

Using the centerline of 253° ± 5° (binned every 1°) for turbine #3 on turbine #1, we calculated power deficits for the nonwake case. For turbine #3 on turbine #1, the nonwake data indicated that turbine #1 produced 17% more power than turbine #3 from the same wind directions. These values probably vary with differing stabilities and wind speeds as well as other factors, but because data to properly stratify them were not available, they were all combined into one case.

For the wake case for turbine #3 on turbine #1 with 5° on either side of the centerline wake, the power deficit of turbine #1/turbine #3 was +3%.

Because the nonwake case indicated that turbine #1 was +17%, this gives a net power reduction of 14% (±5%) for turbine #1 in the wake of turbine #3 at a 10.2-D downwind distance.

The centerline of 276 ± 5° was used for turbine #2 on turbine #1. The nonwake power deficits between turbine #1 and turbine #2 indicated that turbine #1 produced 4% more power than turbine #2 for the same wind directions.

The turbine #2 on turbine #1 wake case illustrated in Figure 4.5 gave a power reduction of 24%, with the net effect of 28% reduction in power for turbine #1 when the differences in the two turbines are taken into account. Figures 4.4 and 4.5 indicate that there was a high degree of scatter in these power ratio calculations, but a net effect is observed in the wake situations.

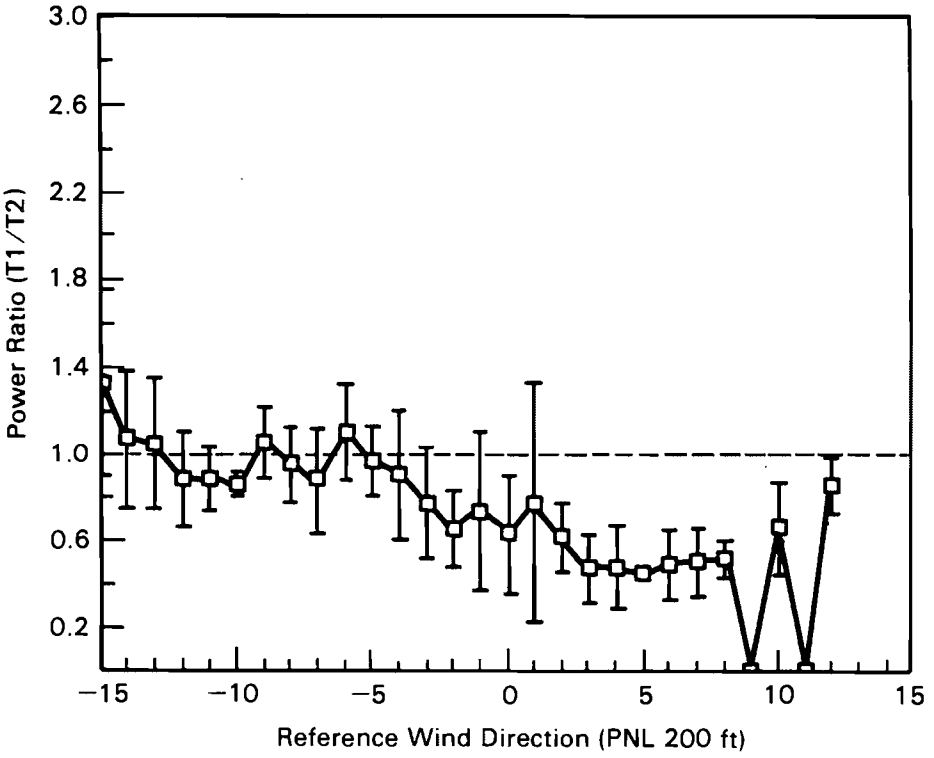

FIGURE 4.5. Power Ratio of Turbine #1 to Turbine #2 as a Function of the Incident Reference Wind Direction (276°) Averaged by 1° Bins. The standard deviations of the ratios are also plotted.

To provide a better picture of the wake and its effects on the downwind turbine, two case studies are shown in Figures 4.6 and 4.7. These cases are both for turbine #2 on turbine #1 at a 6.7-D downwind distance. Figure 4.6 is from November 4, 1982, at 1635 and Figure 4.7 is from November 4, 1982, at 2349 to November 5, 1982, at 0248. One of the interesting features of these two plots is the width of the apparent wake. The centerline of the wake should be at 276° and, by watching the power deficit as the wind direction

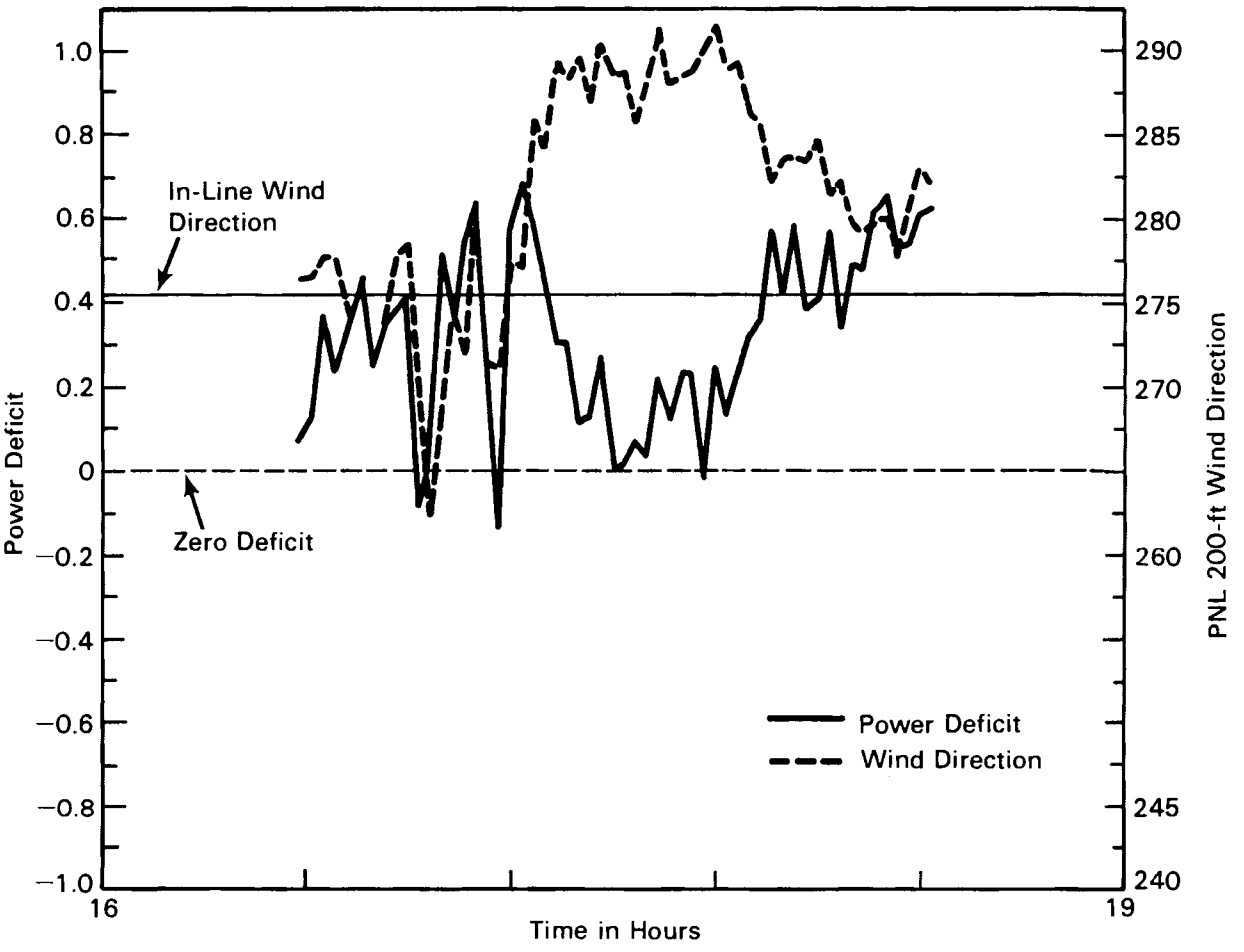

FIGURE 4.6. Time Series of Power Deficit of Turbine #1 to Turbine #2 and PNL 200-ft Wind Direction from November 4, 1982, at 1635 to 1826. Zero deficit and centerline wake direction lines are indicated on the plot.

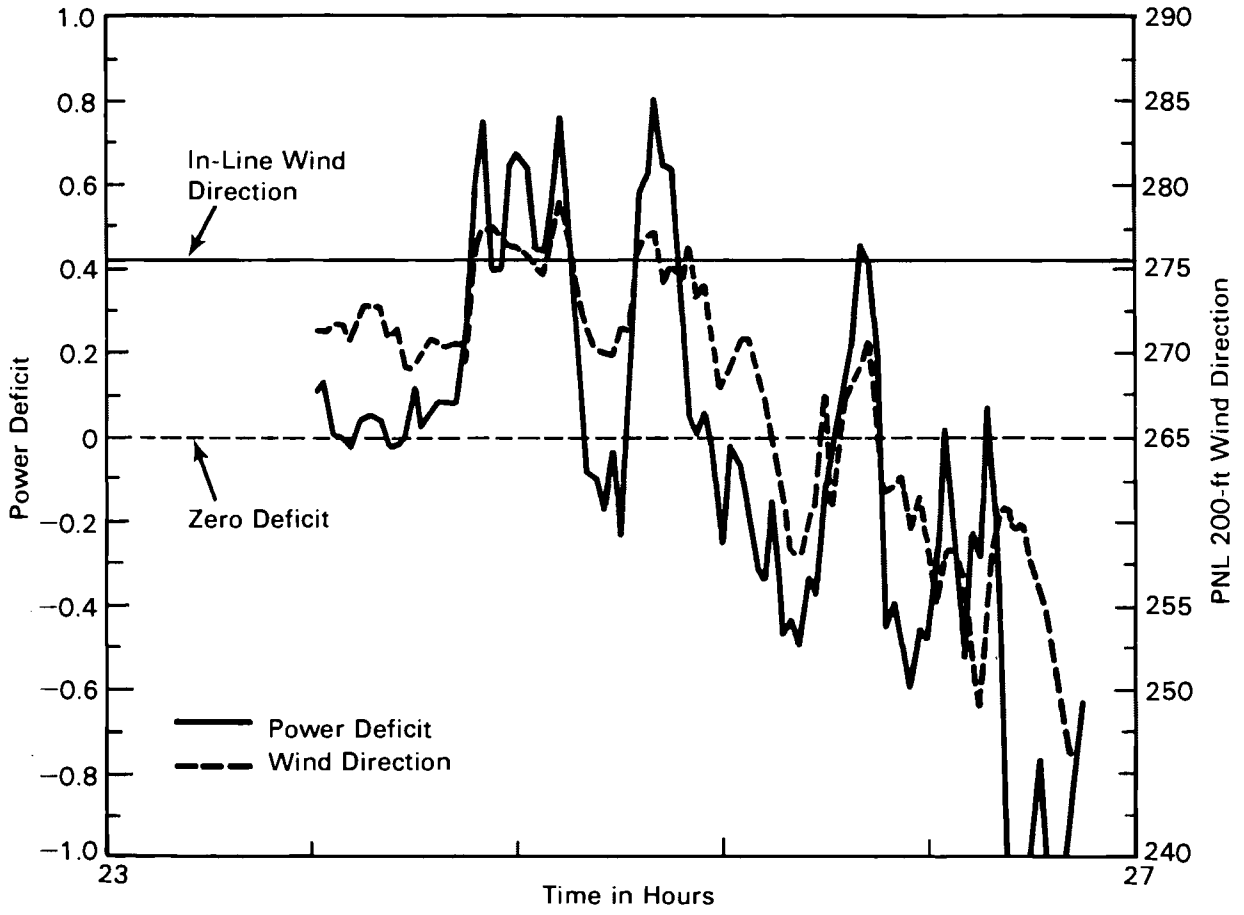

FIGURE 4.7. Time Series of Power Deficit of Turbine #1 to Turbine #2 and PNL 200-ft Wind Direction from November 4, 1982, at 2349 to November 5, 1982, at 0248. Zero deficit and centerline wake direction lines are indicated on the plot.

shifts away from the centerline, one can see that the deficit drops once the wind direction is greater than 282° and less than 272°. These values vary, but, as a whole, these plots indicate a wake width of 8 to 10° for a 6.7-D downwind distance. The power deficits observed in these plots vary from 10 70%; however, these values are not to be used for determining the actual power deficit of the wake but, rather, to show the great fluctuations of the values and to show the difficulty in measuring these wake characteristics accurately.

4.5 VELOCITY RATIOS AS A FUNCTION OF INCIDENT WIND DIRECTION

From the basic data set, August 29 to November 12, it is also possible to summarize observations of turbine wakes on the meteorological towers. The same analytical procedures were used as for the power ratios, only in this case velocity ratios of the tower affected by the wake to the "free-stream" tower were calculated for the various wind direction bins. From Figure 3.2c, it can be seen that use of the meteorological towers provides additional information at different downstream distances from the turbine interaction data, and that different reference wind directions for the wake centerline are necessary. Preliminary results of an analysis of these data were given by Hadley and Renne (1983).

Figure 4.8 shows the velocity ratio when the wake from turbine #1 would be impacting the PNL tower. Under these conditions, the wake centerline would strike the tower for a wind direction of 42°. The figure indicates a maximum velocity deficit of around 50% from the background data. If the nonwake is defined by the far ends of the wake data case, then the maximum wake deficit is around 25% (75% - 50%). However, as shown in Figure 4.1, a portion of this velocity deficit could result from the tower shadow effect on the wind sensors on the PNL and BPA towers. Therefore, these results are not conclusive but are only observations.

Figure 4.9 shows the velocity ratio for cases when the PNL tower is expected to be in the wake of turbine #3. This represents a downwind distance of 8.3 D, requiring the incident wind direction of 260° for the wake center to impact on the tower. A 30% velocity deficit is obtained if the wake data deficit is subtracted from the ambient data. If the edges of the wake data

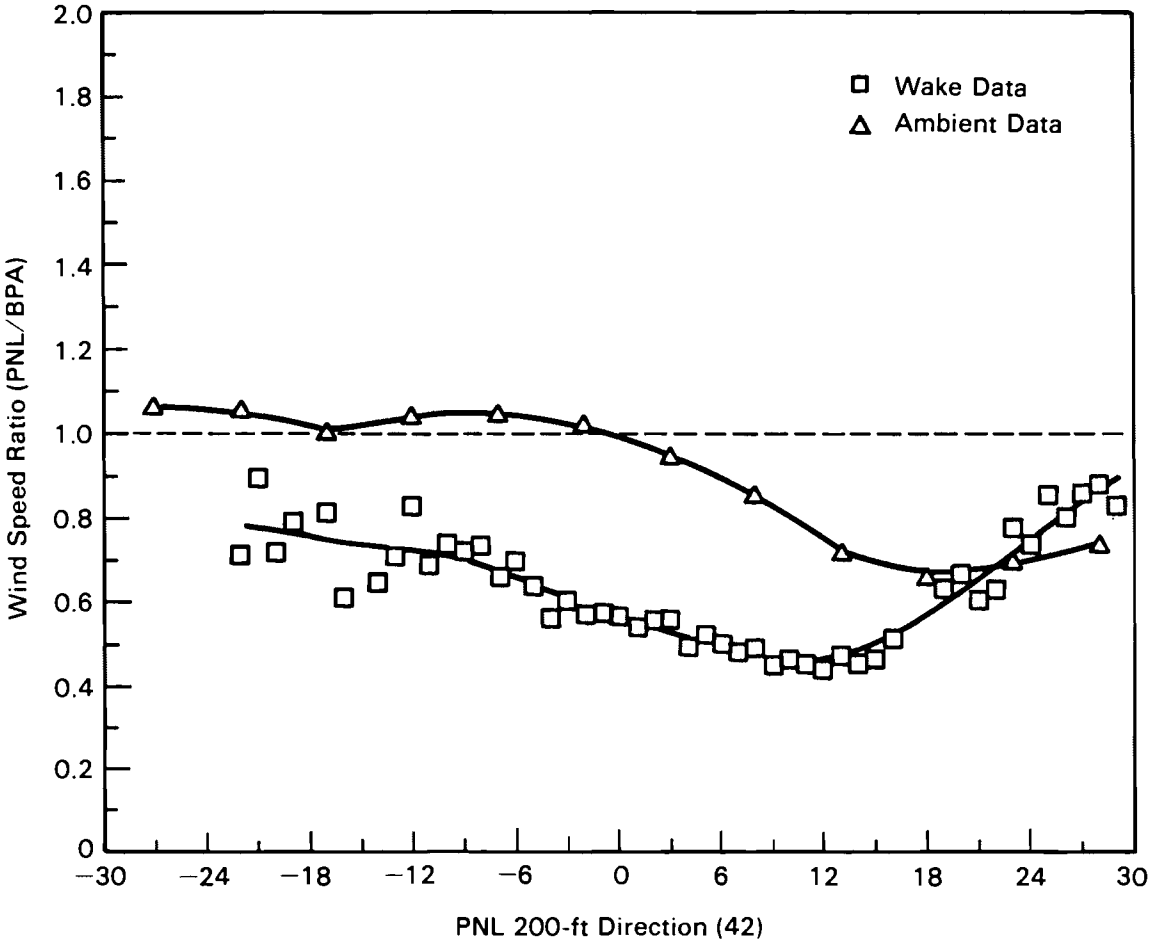

FIGURE 4.8. Velocity Ratio (200 ft PNL/195 ft BPA) as a Function of Incident Reference Wind Direction (42°) Averaged by 1° Wind Direction Bins when in the Wake of Turbine #1.

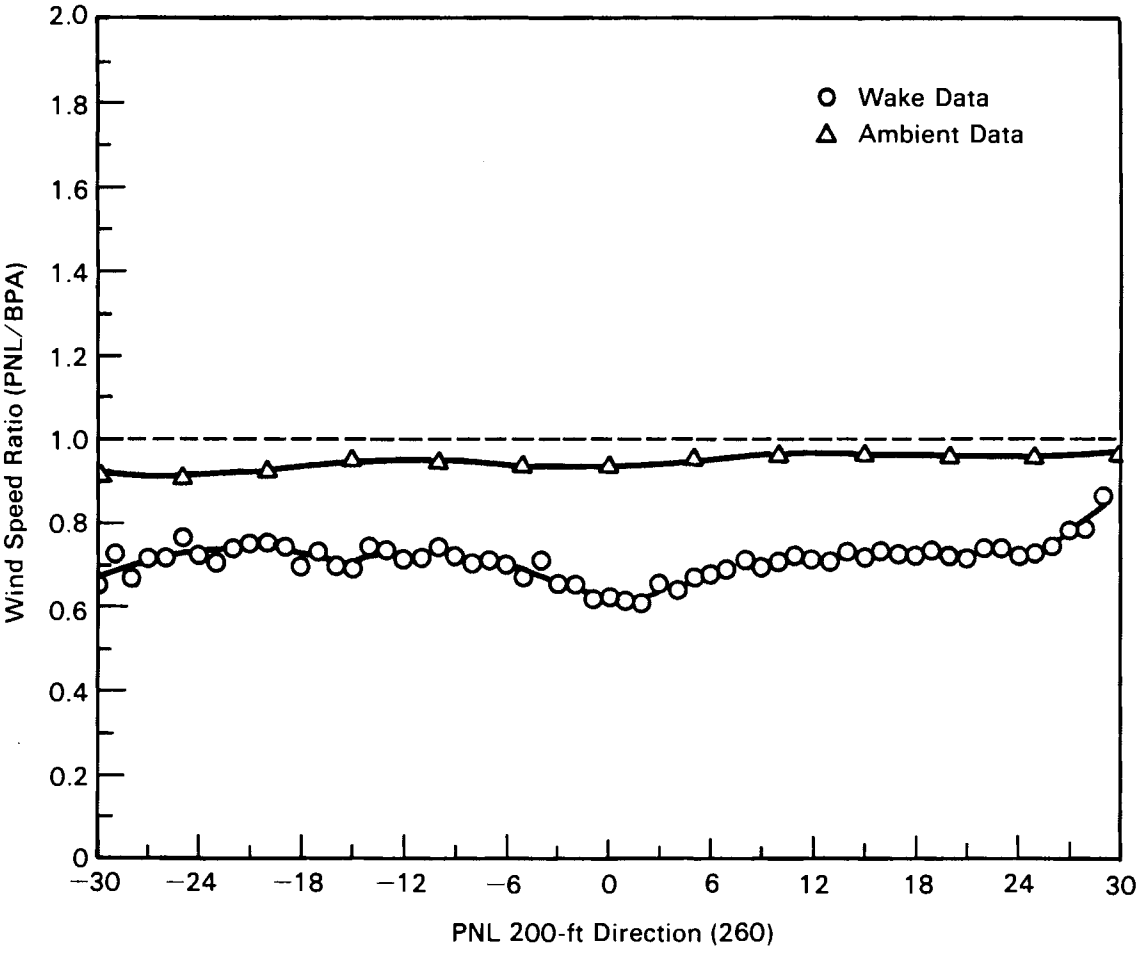

FIGURE 4.9. Velocity Ratio (200 ft PNL/195 ft BPA) as a Function of Incident Reference Wind Direction (260°) Averaged by 1° Wind Direction Bins When in the Wake of Turbine #3.

are used as the nonwake deficit, a maximum velocity deficit of 15% (75% - 60%) is observed. Why the velocity ratios of the ambient and the edges of the wake data case vary so much is unknown; at this time the authors cannot give a confident explanation of this phenomenon.

The available data were insufficient to identify wake effects on other machine/tower configurations using this statistical averaging technique. However, an interesting case study was identified when the BPA tower was in the wake of turbine #3 just as the machine went through a startup cycle. The BPA tower is only 1.7 D downstream of turbine #3 for a wind direction of 207°. Figure 4.10 provides a time series of turbine #3 power and the "free stream" wind direction (obtained from the PNL tower) for this case, which occurred at 0930 on October 22. During this period of time, 5-s data samples were being recorded, but 2-min averages were calculated for the time series representation. The figure shows that at the time of machine startup, about 7 min into the series, wind directions were shifting from about 200° to about 185°. After about 40 min the winds gradually shifted back to around 200°. Figure 4.10 also shows the effect of this activity on the wind speed measured at the BPA 195-ft level. The PNL wind speed and wind directions are included for comparison. Immediately after startup, the BPA wind speed dropped from almost 15 mph to less than 3 mph, a reduction that far exceeds what would be expected in the near wake from simple axial momentum theory. The velocity deficit remained at this low value for about 10 min. Then, with the winds still blowing from the south, the velocity ratio increased to about 0.4, which is what would be expected in the near wake of the turbine at maximum C_p. Eventually, the wake moved completely away from the tower, and the velocity at the BPA tower approached that at the PNL tower.

One explanation for this extremely low velocity ratio is that the wind directions in the wake were also highly fluctuating. Since the BPA tower is equipped with propeller-type sensors, they could have been experiencing excessive "vaning" during this period, which would result in lower measured wind speeds.

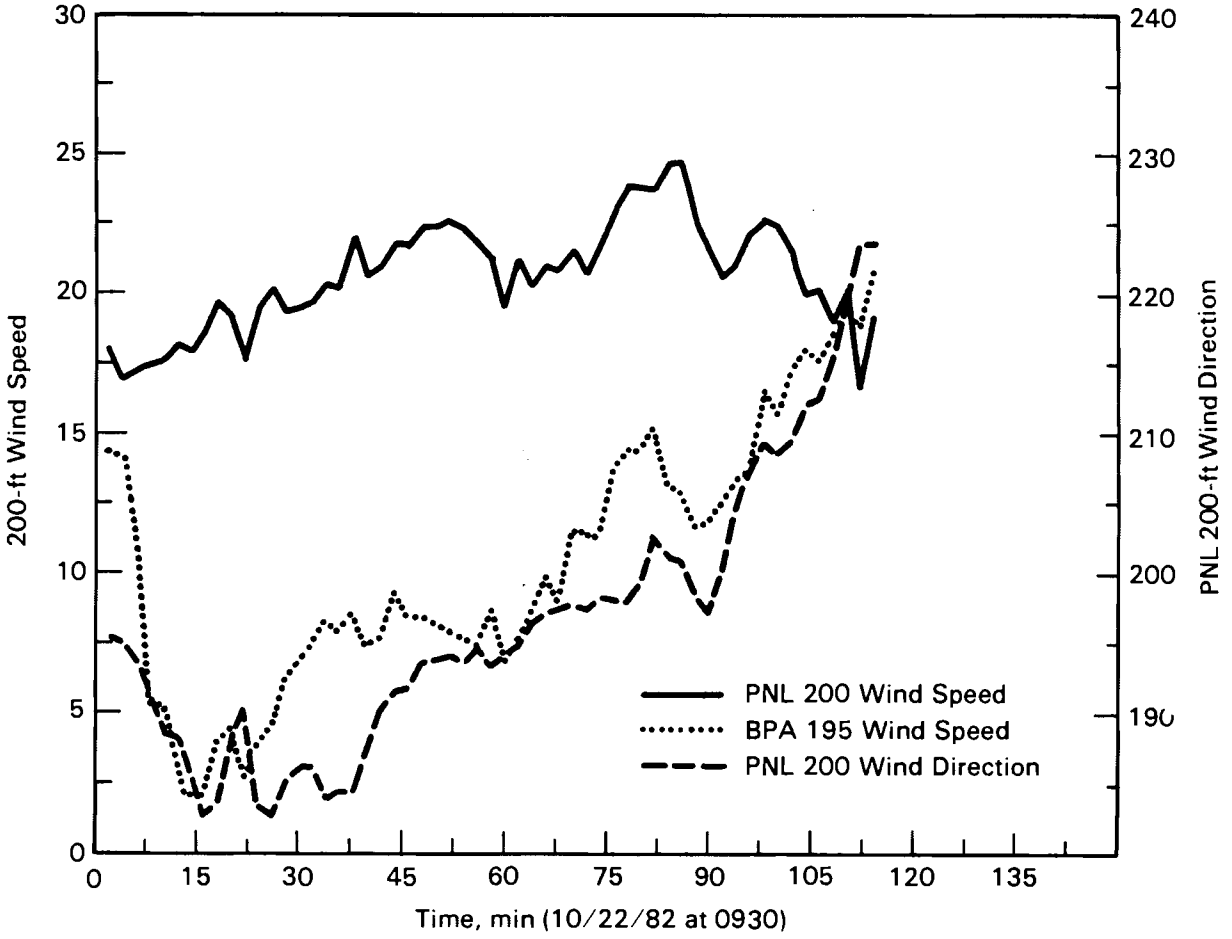

FIGURE 4.10. Wind Speeds at 195-ft BPA and 200-ft PNL Versus PNL Wind Direction as a Function for Time in Minutes Starting at 0930 on 10/22/82 When the BPA Tower Was in the Wake of Turbine #3 (1.7 D).

4.6 EXAMINATION OF PARAMETER VARIATION ON WAKE EFFECTS

The variation of wake effects for different stability, wind speed (or power output), time averaging, and turbulence intensity categories was examined. Since these parameters could be studied only for those wind directions that would place the downwind tower or turbine in a wake centerline, data were limited for the various categorizations. In fact, unstable conditions existed for over 95% of the available data, so that a stratification according to stability class was not possible. (Hadley and Renne (1983) presented some

preliminary results of velocity deficit measurements according to a stability classification. Despite the limited data, their results indicate that velocity deficits in the wake are less for unstable conditions than for stable conditions).

Examining wake effects under varying wind speed conditions allows us to test the hypothesis that the terrain at Goodnoe Hills has some effect on the wind flow and, as a result, on the wake. Therefore, wake profiles were developed for different MOD-2 power classes, which represent different wind speed classes: 0.5 to 1.0 MW; 1.0 to 1.5 MW; and 1.5 to 2.5 MW. The results are shown in Figure 4.11. This figure should be compared with Figure 4.4, which present the power ratio of turbine #3 to turbine #1 versus reference wind direction (253°) for all power classes. Figure 4.4 indicated the wake centerline to be at -4° (south of predicted centerline) with a maximum power deficit of 20%. Figure 4.11a shows the same analysis for power class of 0.5 to 1.0 MW (low wind speeds). The actual centerline of the wake seems to be at -8° with a power deficit of 25%. Figure 4.11b is for 1.0 to 1.5 MW power, or medium wind speeds, and indicates a wake center at -4°, while Figure 4.11c (1.5 to 3.0 MW, or high wind speeds) indicates the wake center is at 0°.

These results suggest that at lower wind speeds or power production classes the wake center tends to meander toward the south. As the wind speeds increase, the center of the wake tends to fall more toward the predicted wake center. These observations indicate the terrain has greater effect on wakes at lower wind speeds. For lower wind speeds, surface friction can cause the winds to be diverted towards the downslope side of the terrain, which would be toward the south.

A case study of turbine #1 in the wake of turbine #3 is shown in Figure 4.12. The period of the data is from September 26 at 2146 to September 27 at 0724; this is about 9 h of continuous 2-min-averaged data. This case indicates a minimum power ratio between turbine #1 and #3 of 0.96 and a normal ratio of 1.08. If the dip in the curve is related to the wake of turbine #3, the averaged wake shows a centerline power deficit of 12%, a width of 15° and a wake centerline offset toward the south by 3°. This compares with a 22% power deficit and a width of about 30° when all the data were used (Figure 4.4).

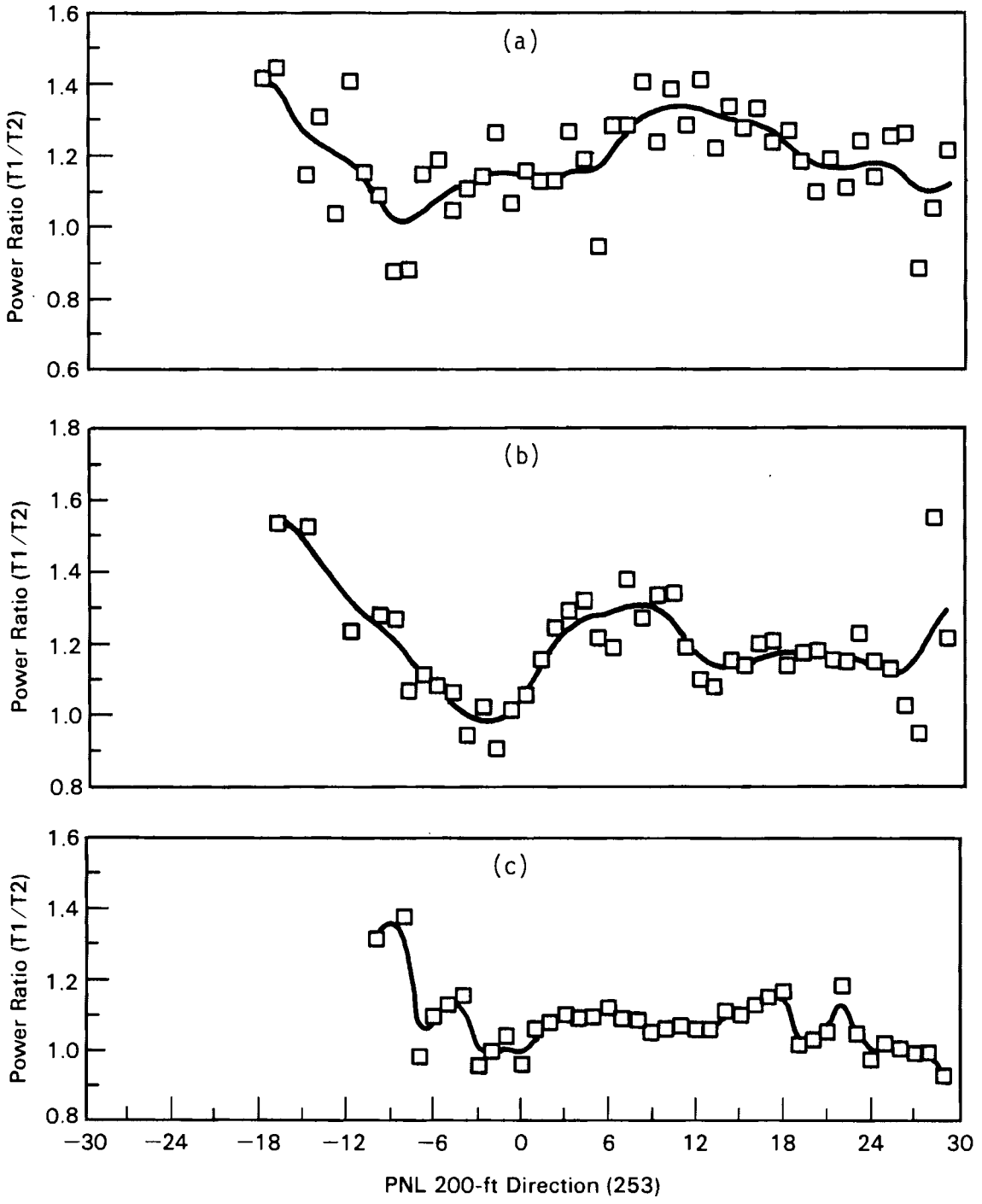

FIGURE 4.11. Power Ratio of Turbine #1 to Turbine #3 as a Function of Incident Reference Wind Direction (253°) and for a Range of (a) Turbine Power 0.5 to 1.0 MW; (b) 1.0 to 1.5 MW; (c) 1.5 to 2.5 MW

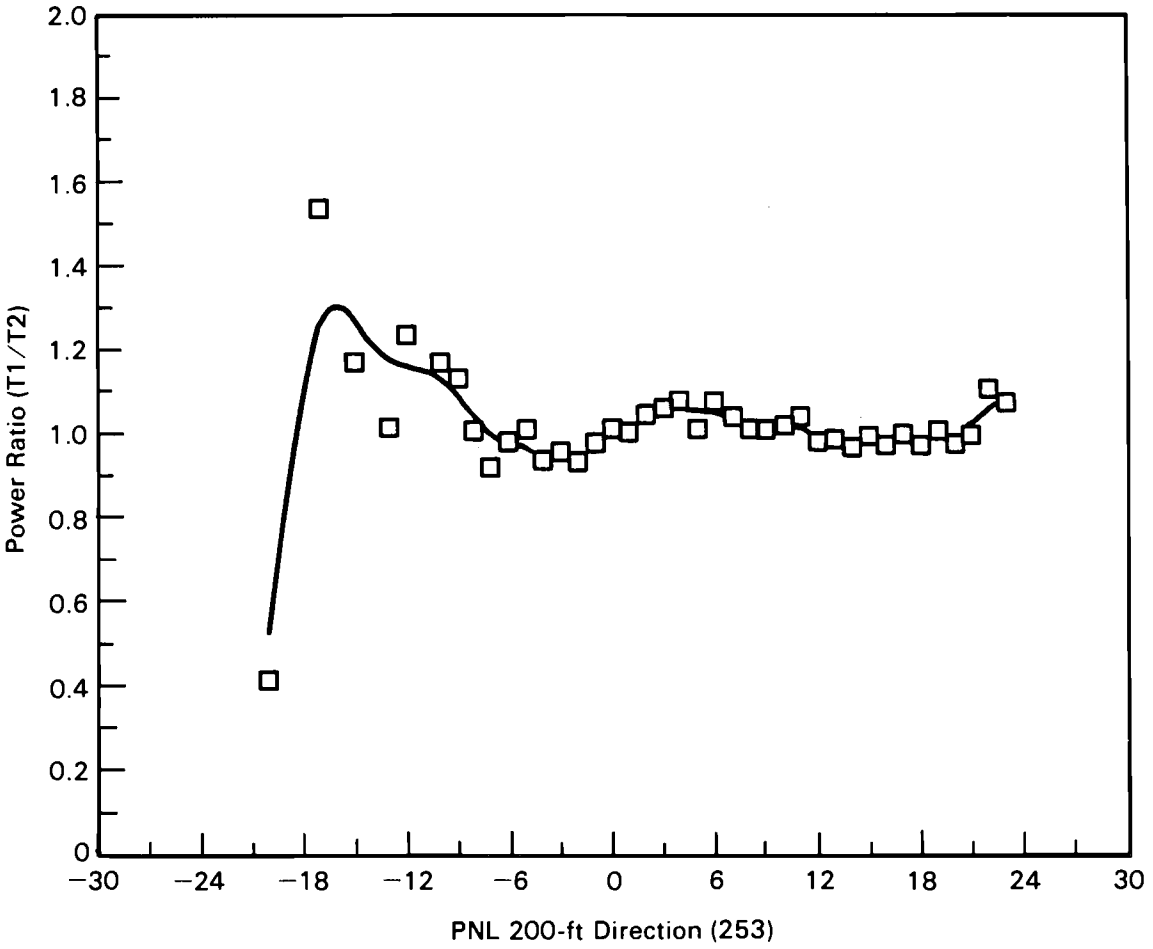

FIGURE 4.12. Power Ratio of Turbine #1 to Turbine #3 as a Function of Incident Reference Wind Direction (253°) for a 9-h Case of Continuous 2-min-Averaged Data (2146 on 9/26/82 to 0724 on 9/27/82).

The data for this case were then re-examined using 10-min averages (Figure 4.13). This figure shows a minimum power ratio of 0.91, with a normal ratio around 1.06. No significant difference in the width and centerline offset is observed using this different averaging time, indicating good agreement between the 10- and the 2-min-averaged data.

A case when turbine #1 was in the wake of turbine #2 was also examined. The case was for 1617 to 1826 on November 4. The results for 2-min and 10-min

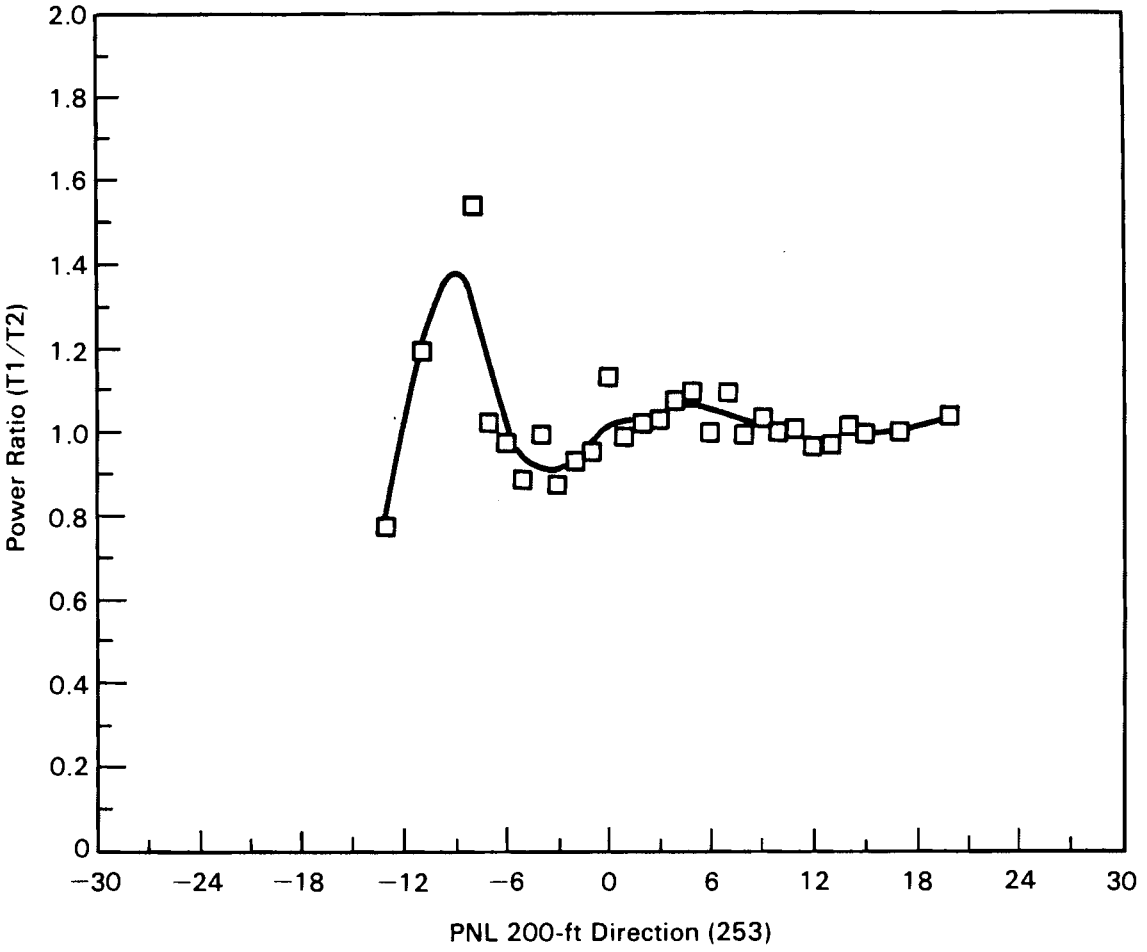

FIGURE 4.13. Same as Figure 4.12 Except the Data Has Been Averaged for 10 min.

averaging are shown in Figures 4.14 and 4.15, respectively. They can be compared with Figure 4.5, which showed the average ratio for the entire data set. Figure 4.5 had shown that the power deficit near the wake centerline was as high as 50%. The average wake centerline appeared to be offset toward the north by about 5°. The width of the deficit was about 20°. Sampling of machine/machine interactions is limited in this case for winds north of 280° because of lack of data.

Figure 4.14 shows the results of the 2-min averaging for the 2-h case study. This case indicates a power deficit of 45%, a width of about 20°, and a centerline shifted about 4° to the north of the reference wake centerline of 276°. These values correspond closely to the values obtained from Figure 4.5. Figure 4.15 shows the result of 10-min averaging for the same case as

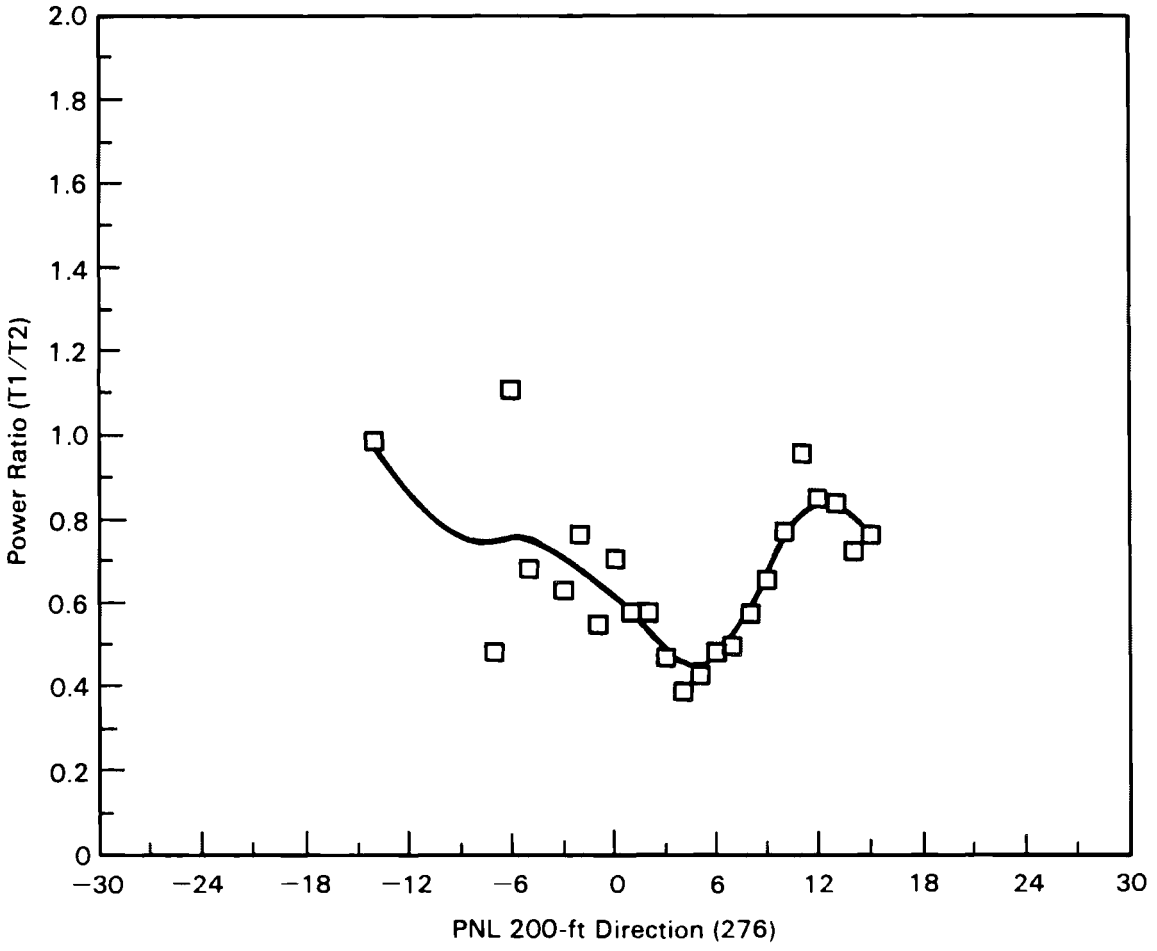

FIGURE 4.14. Power Ratio of Turbine #1 to Turbine #2 as a Function of Incident Reference Wind Direction (276°) for a 2-h Case of Continuous 2-min-Averaged Data (1617 on 11/04/82 to 1826 on 11/04/82).

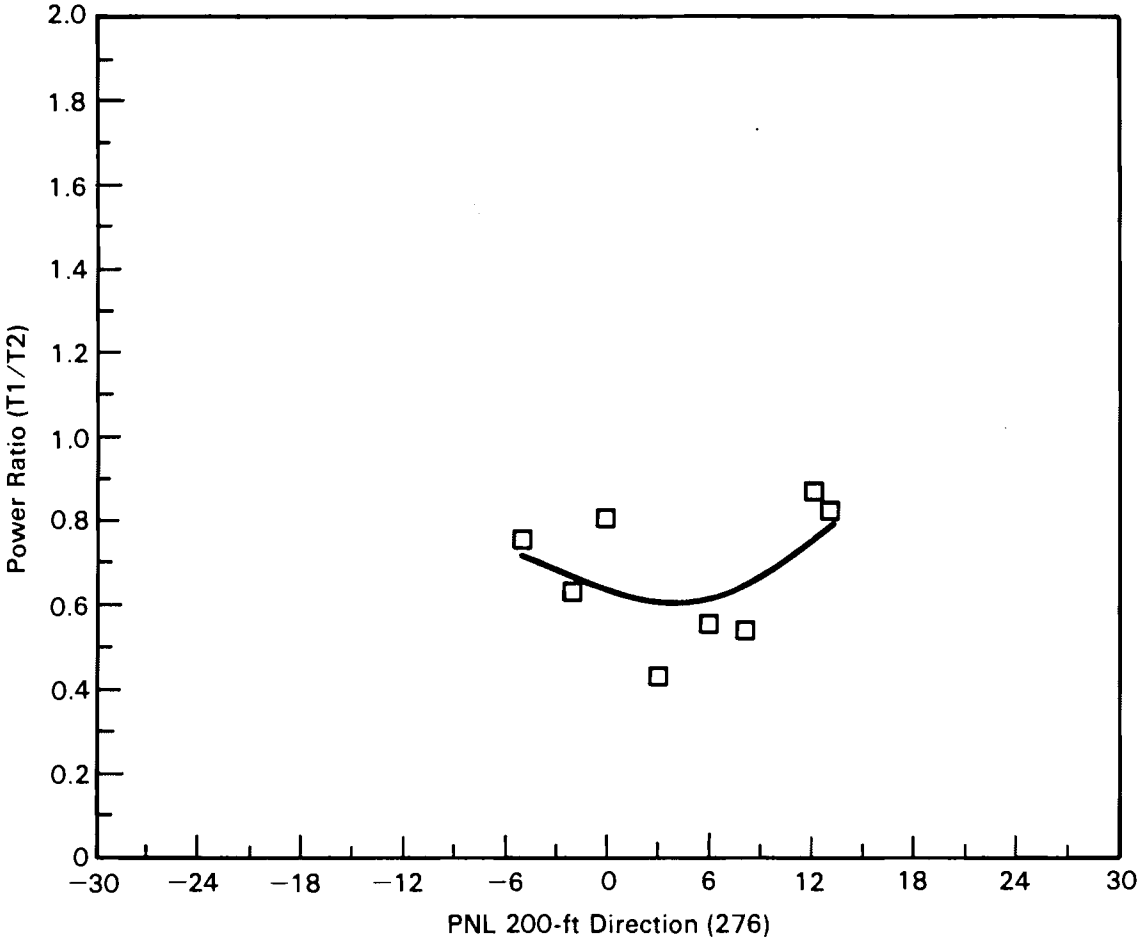

FIGURE 4.15. Same as Figure 4.14 Except the Data has been Averaged for 10 min.

Figure 4.14. There are too few data to establish a representative width, but the northward shift of the wake centerline, in this case by about 6°, is still evident. The power deficit still appears to be about 50% if a normal ratio of 1.0 is assumed. Thus, there does not appear to be a significant effect on our conclusions using two different time-averaging schemes for these case studies.

The full data set was also stratified according to turbulence intensity categories. Turbulence intensity, I_t, is defined as:

$$I_t = \frac{\sigma_U}{\bar{U}} \tag{4.1}$$

where σ_U is the standard deviation of the 1-s values for a given 2-min wind speed average, and $\bar{U}$ is the average 2-min wind speed. The data were sorted into two categories: high turbulence intensity (>0.1), and low turbulence intensity (<0.1). Table 4.4 gives the minimum observed velocity and power ratios for various machine/machine or machine/tower wake interactions. The results of the table show that the velocity ratio is more influenced by turbulence intensity than the power ratio, particularly close to the near wake. For low turbulence, the momentum deficit is higher (velocity ratio lower), because of the limited mixing of ambient air in the wake. This is not discernible from the power ratios, however, since turbine power output is a large "filter" of wind speed values.

4.7 OBSERVATIONS OF TURBULENCE IN THE WAKE

The importance of turbulence characteristics in wakes cannot be understated. Wake-induced turbulence could have an impact on the structural integrity of the machine that would have not been anticipated from free-stream background measurements. In addition, the lateral turbulence characteristics of the wake control its growth and dissipation, which are important when planning large wind turbine farms.

A limited amount of turbulence level information is available from the August 29 to November 12 data set. The actual turbulence level can be

TABLE 4.4. Minimum Velocity and Power Ratios for Two Turbulence Intensity Categories. Velocity Ratios are PNL/BPA Towers; Power Ratios are Turbine #1/Upwind Turbine.

Downwind Wake Distance, D	Velocity Ratios		Power Ratios	
	Low I_t (<0.1)	High I_t (>0.1)	Low I_t (>0.1)	High I_t (>0.1)
8.3 (Turbine #3 on PNL)	0.79	0.83	--	--
2.2 (Turbine #1 on PNL)	0.52	0.62	--	--
6.7 (Turbine #2 on Turbine #1)	--	--	0.76	0.78
10.2 (Turbine #3 on Turbine #1)	--	--	1.01	0.96

parameterized by the 1-s standard deviations of the 2-min wind speeds, which provide a better representation of turbulence level in the wake than turbulence intensity; this is because in the wake the lower mean velocity can raise the value of turbulence intensity without indicating whether actual turbulence has increased.

Cases when the wake of turbine #3 impacted the PNL tower (a downwind distance of 8.3 D for a wind direction of 260°) were analyzed. Figure 4.16 shows the average turbulence levels for the various incident wind directions referenced to the 260° centerline value. The figure shows turbulence levels for each of three levels on the PNL tower: 50, 200, and 350 ft. No change in turbulence in the wake centerline is detected at the 50-ft level. However, a slight increase is discernible at the 200-ft level, and for winds more southerly than 260° at the 350-ft level. General turbulence levels are expected to be higher for southwesterly winds, because of the topography of the Columbia River gorge. However, except for the slight increase observed at the 200-ft level, no firm evidence regarding wake-induced turbulence can be obtained from Figure 4.16.

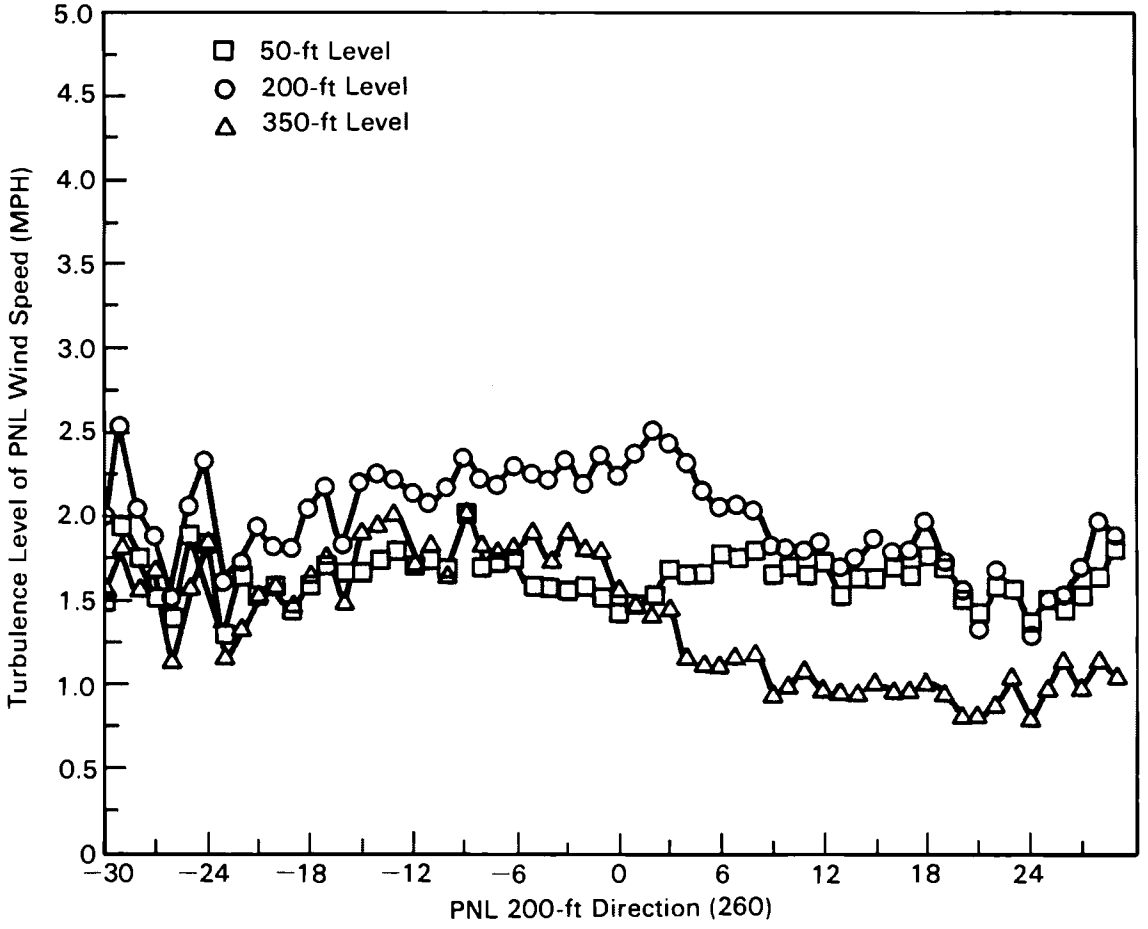

FIGURE 4.16. Turbulence Levels of PNL Wind Speed as a Function of Incident Reference Wind Direction (260°)

5.0 GENERALIZED WAKE CHARACTERISTICS AT GOODNOE HILLS

5.1 COMPOSITE WAKE STRUCTURE

In this chapter, we assemble the information developed in the previous chapter on wake characteristics from machine/machine and machine/tower interactions at Goodnoe Hills into a composite structure of the wake. We compare this composite wake with some common numerical models of wind turbine wakes and with some previous observational studies of wakes performed at Goodnoe Hills.

The structure of the composite wake is presented in two ways. In one presentation, the ratio of the power of the downwind turbine to the upwind turbine is shown for various tip speed ratios and various downwind distances. The tip speed of the MOD-2 is 186 mph, and the tip speed ratio is defined as the tip speed divided by the free-stream velocity at 200 ft. Data from the meteorological towers are included in these analyses by converting their velocity ratios to power ratios using a method described below. In the second presentation, the ratio of the velocity measured at the meteorological tower in the wake to that measured at the tower in the free stream is shown for various turbine tip speed ratios and downwind distances. In this case, the machine/machine interaction data are included in the analysis by converting turbine power output to effective wind velocity, using the method described below.

The power ratios for machine/machine interactions are a straightforward calculation for this analysis. However, there are only sufficient data to examine centerline wake deficits for two tower configurations: turbine #2 on turbine #1 (6.7 D), and turbine #3 on turbine #1 (10.2 D). In order to obtain a more complete composite wake analysis, power ratios were also calculated for machine/tower interactions, where the 200-ft level wind speed of the tower in the wake of a machine was compared with the free-stream wind speed measured at the other tower at the same level. These wind speed ratios had to be converted to power ratios to be compatible with the machine interaction cases. This conversion was accomplished using a fourth-order polynomial developed from the power curve of turbine #3 shown in Figure 4.2. Data from the BPA tower at the 195-ft level were used for wind speed. This turbine/tower combination was

used since it had the most data available for developing the relationship. The resulting power output equation for this is

$$P = 1.06 - 0.22V + 0.15V^2 - 2.3 \times 10^{-4}V^3 \qquad (5.1)$$

where P is power in MW and V is velocity in mph.

Equation (5.1) was applied to the upstream and in-wake velocity observations for all cases where one of the meteorological towers was in the wake of a turbine. Inclusion of data from these cases provided two additional downwind distances from which to develop the composite wake structure: 2.2 D, where turbine #1 produced a wake on the PNL tower; and 8.3 D, where turbine #3 produced a wake on the PNL tower. There were insufficient data from the August 29 to November 12 period to obtain wake characteristics at other downwind distances possible at the Goodnoe Hills array.

The velocity ratios were also calculated for this same data set. In this case, calculation of velocity ratios from the wakes and free-stream tower was straightforward, but calculation of velocity ratios from turbines required a conversion of turbine power output to wind speed. This conversion was established from the same data used to obtain Equation (5.1). In this case, velocity is the dependent variable, and the fourth-order polynomial becomes

$$V = 11.8 + 10.7P - 3.34P^2 + 1.05P^3 \quad . \qquad (5.2)$$

Figure 5.1 shows the power ratio as a function of tip speed ratio for the four downwind distances. No adjustment to differences in power-producing characteristics of the turbines (Section 4.2), or to differences in wind speed measurements at the towers (Section 4.1), was made. Such adjustments could affect the relative position of the profiles to each other, but would not affect the shape of each profile. The data making up these profiles include only those cases where the incident wind direction is within ±5° of that necessary for the wake centerline to impinge on the downwind turbine or tower. A tip speed ratio bin width of 1.0 was used for sorting the data, with each bin centered over the integer value of tip speed ratio.

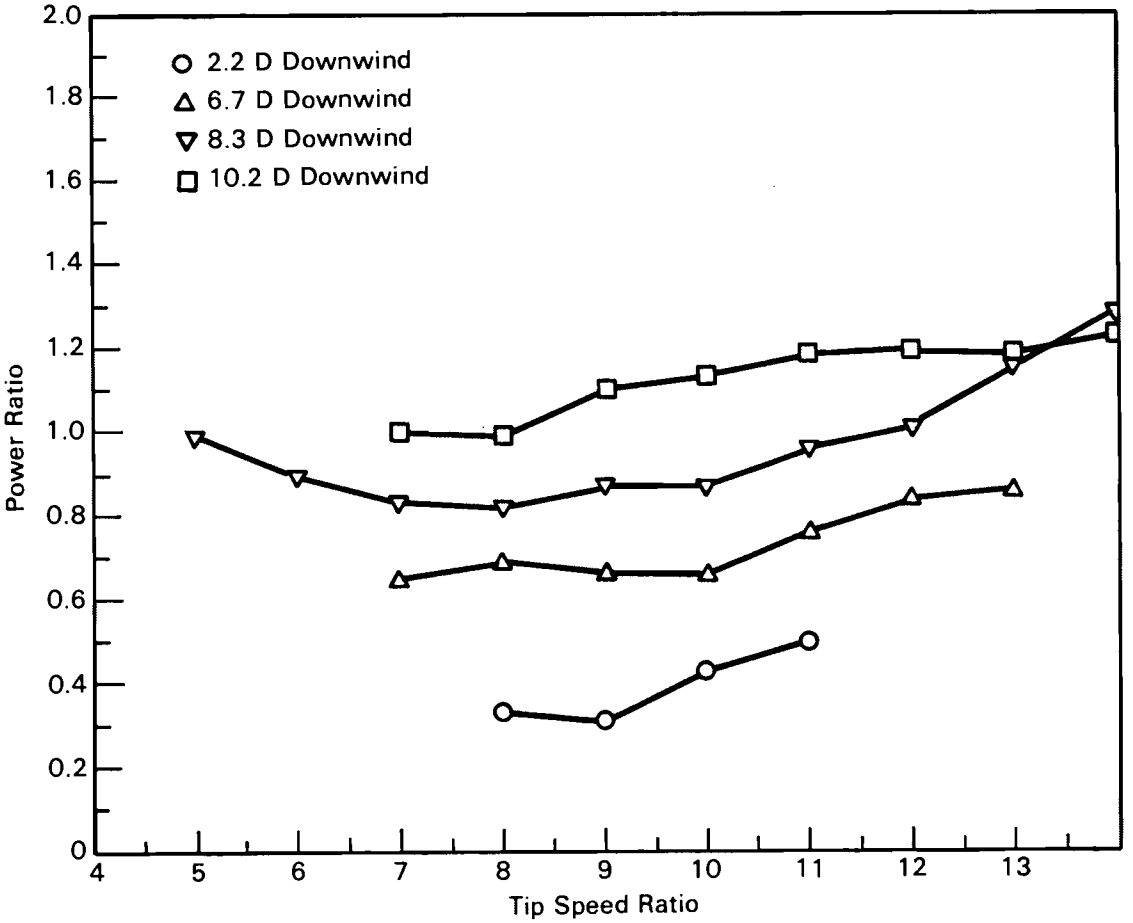

FIGURE 5.1. Power Ratios as a Function of Tip Speed Ratio for Four Downwind Distances.

Figure 5.2 shows the velocity ratio as a function of tip speed ratio for the same four downwind distances. The shapes of the profiles are essentially the same as those in Figure 5.1. The four profiles are concentrated more closely to the 1.0 value than the power ratios, indicating that as wind speed varies, turbine power output varies proportionately more, which is to be expected.

Figures 5.1 and 5.2 both show that the minimum power ratio (i.e., maximum wake effect) generally occurs for tip speed ratios between 7 and 9. It is of interest to compare this result with Figure 5.3, which shows the actual power coefficient, C_p, curve for the MOD-2 as a function of tip speed ratio. This figure shows that the machine's maximum C_p occurs at a tip speed ratio of 8.4. From this experimental C_p curve, we can apply the axial momentum theory to

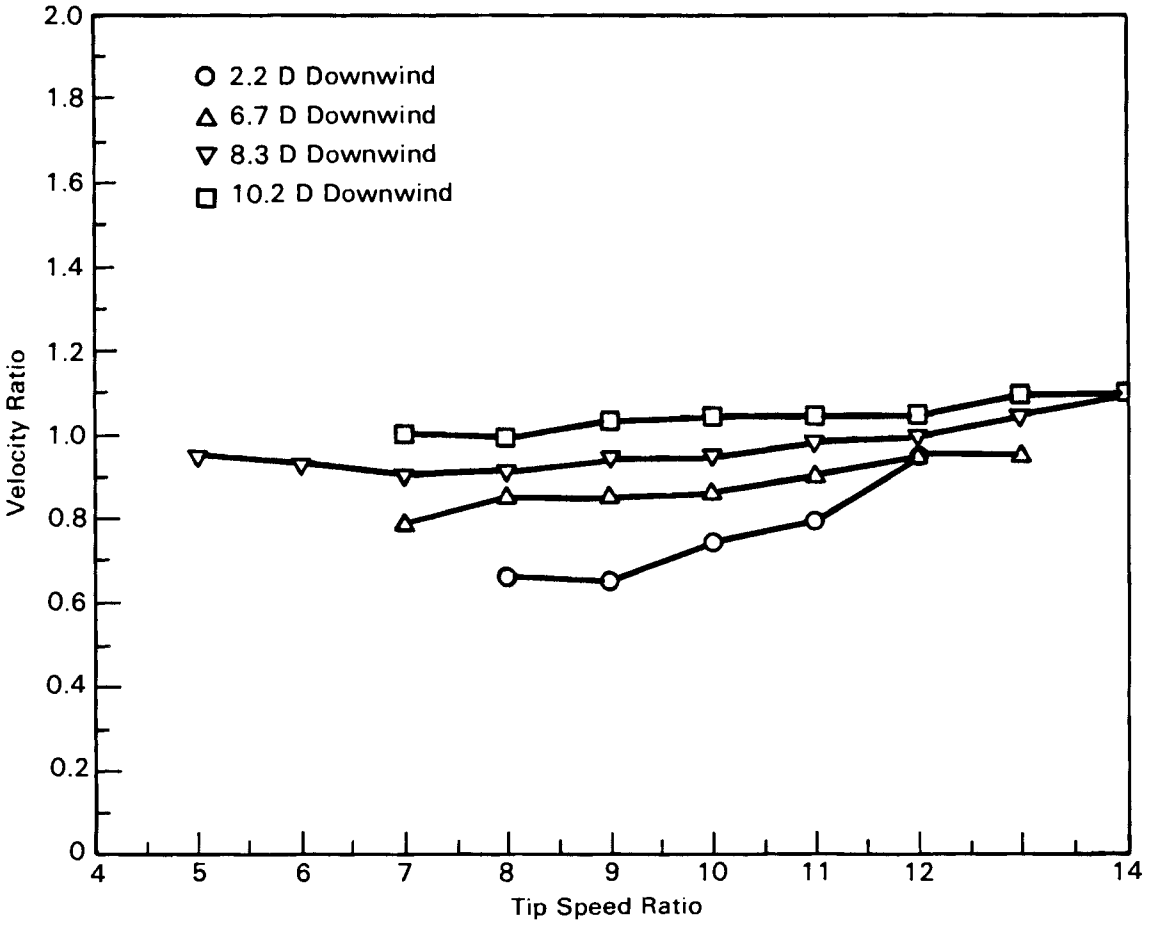

FIGURE 5.2. Velocity Ratios as a Function of Tip Speed Ratios for Four Downwind Distances

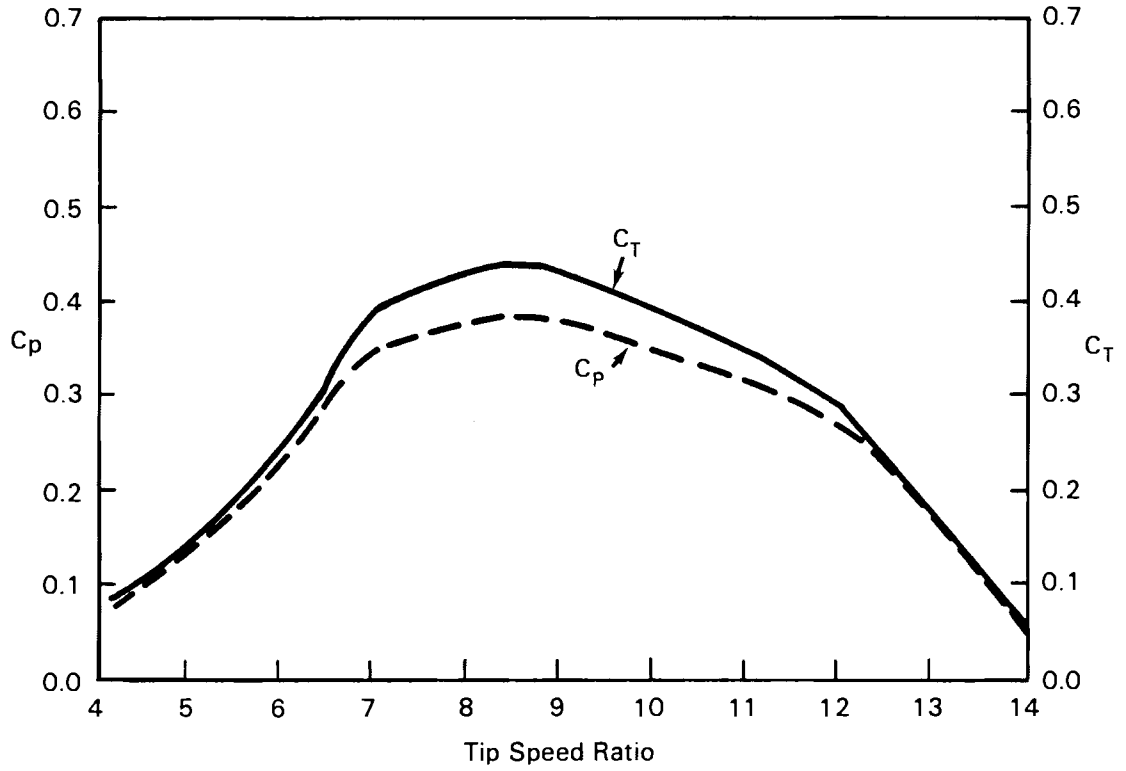

FIGURE 5.3. Actual Power Coefficient and Trust Coefficient Curve for the MOD-2 as a Function of Tip Speed Ratio

obtain the thrust coefficient, C_T. This is done by combining Equations (2.5), (2.8) and (2.9), and defining the term $m = u_o/u_f$ to obtain

$$C_p = 1/2(1 + 1/m - 1/m^2 - 1/m^3) \quad . \tag{5.3}$$

The term m is then solved for the values of C_p given in Figure 5.2. Then C_T is determined from Equation (2.13). These values of C_T are included in Figure 5.3 and show that C_T varies according to the experimental C_p curve. Therefore, the downwind momentum deficit would be largest (power and velocity ratios lowest) at the maximum value of C_p. The results in Figure 5.1 are consistent with this conclusion. This can easily be explained on physical grounds: at the maximum C_p, and therefore maximum C_T, the efficiency of the machine to

extract energy from the air is highest. As the C_p decreases, more of the incoming available energy is "spilled" into the downstream flow by the rotor, increasing the wind velocity of the wake.

Figures 5.1 and 5.2 also show the progressive decay of the wake (i.e., increase in power and velocity ratios) with increasing downwind distance over the entire range of tip speed ratios. This can be seen more clearly in Figure 5.4, which shows the downwind power ratio, and Figure 5.5, which shows downwind velocity ratios for four different tip speed ratios. The lowest power ratios are near the region of maximum rotor efficiency of the MOD-2 (tip

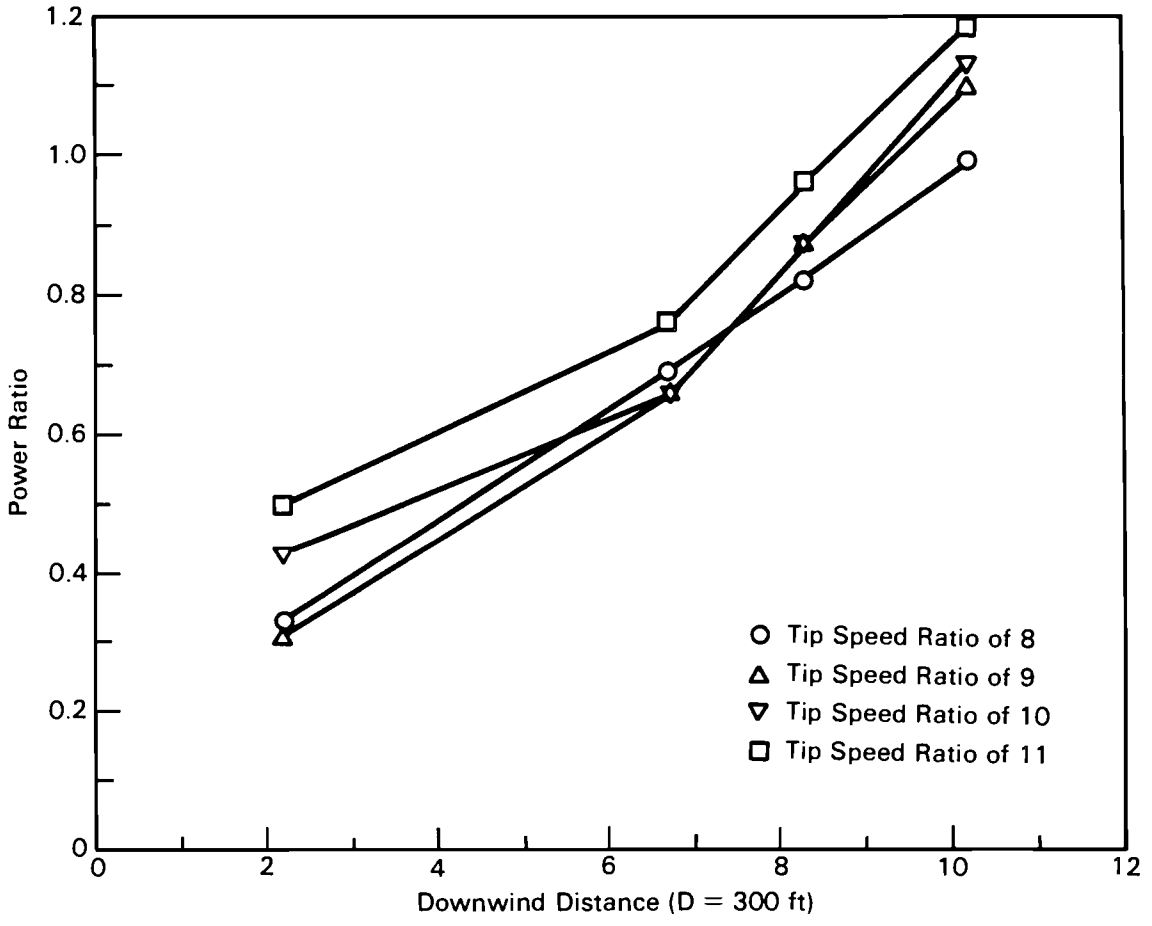

FIGURE 5.4. Power Ratio as a Fuction of Four Downwind Distances for Given Tip Speed Ratios

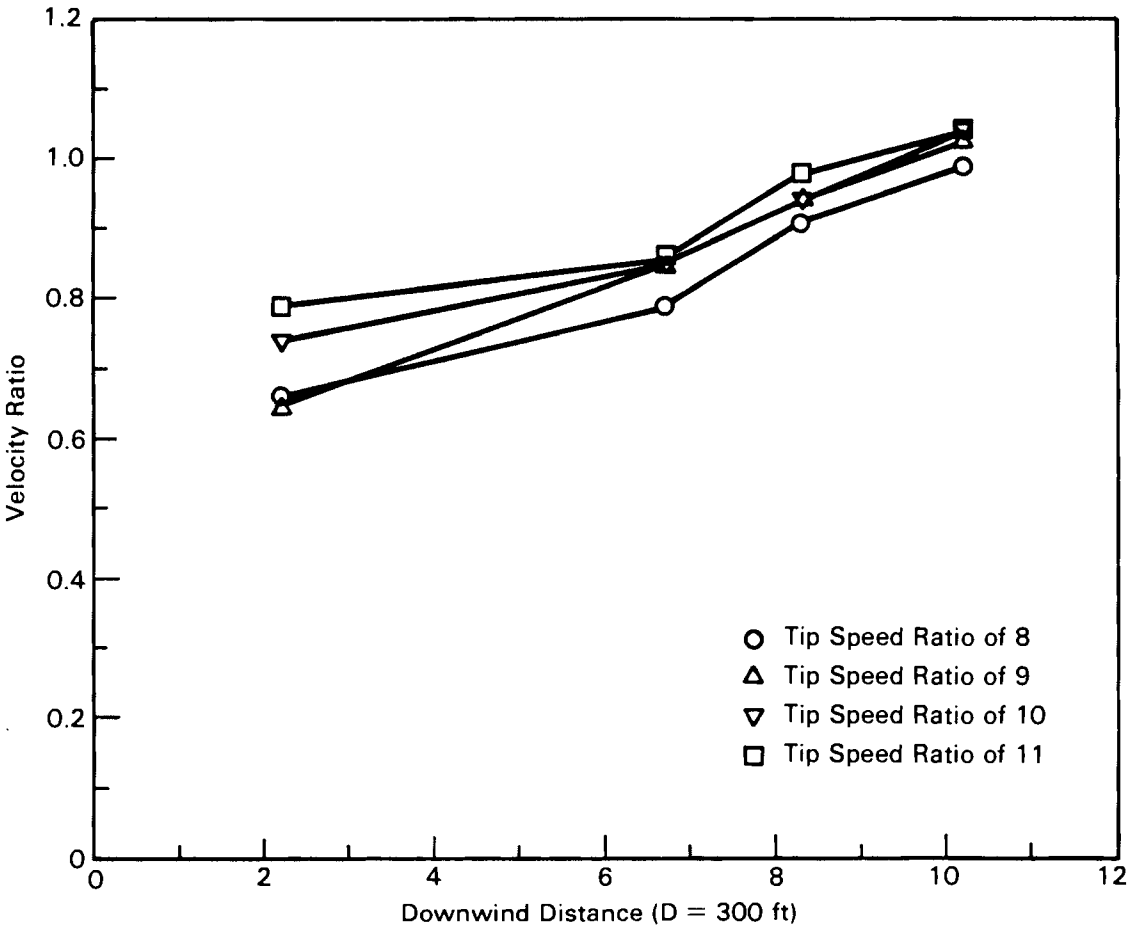

FIGURE 5.5. Velocity Ratio as a Function of Four Downwind Distances for Given Tip Speed Ratios

speed ratio of 8.4). Although little can be said about the shape of the profiles, since each curve is made from two different calculation procedures (machine/machine and machine/tower interactions), they do indicate that at 2.2 D, near-wake conditions exist, while at the other downwind distances where the power and velocity ratios rapidly increase, far-wake conditions exist. In addition, the more rapid recovery of the wake occurs at the higher tip speed ratios. This is expected, since a weaker near wake is established by the lower thrust coefficient, and the lower wind speeds allow for more complete dissipation because of the increased turbulence levels at any given downwind distance.

5.2 COMPARISON WITH NUMERICAL MODELS

Although a number of numerical wake models have been developed over the past decade, none have been given as wide attention as the one developed by Lissaman (1977). This model was recently revised and tested for the machine configuration and meteorological conditions at Goodnoe Hills (Lissaman, Gyatt and Zalay 1982). The revised version of the model is used as a comparison against the composite wake shown in the previous section.

The near wake of the model is determined from the turbine thrust coefficient by the relation (see also Equation [2.13])

$$m = u_o/u_f = (1 - C_T)^{0.5} \quad . \qquad (5.4)$$

In the far-wake region, the growth and dissipation of the wake are governed by the ambient transverse turbulence intensity. Lissaman, Gyatt and Zalay equate this term to the measured turbulence intensity multiplied by a factor of 0.6. Since the data with which model comparisons are being made encompass a wide variety of turbulence intensities, the model will be calculated for a range of representative values.

Baker and Walker (1982) present a simpler version of a numerical wake model. Their model is based on considerations derived from the axial momentum theory presented in Chapter 2. Their "simplified wake model" for the wake centerline velocity deficit is given as

$$u_o/u_f = \frac{0.3780C_T^{1/3}}{(Bx/D)^{2/3}} \qquad (5.5)$$

where B is an empirical parameter for the transverse turbulence intensity. A relation for B was developed from a theoretical argument that transverse turbulence intensity, I_V, can be depicted from a measure of the fluctuations of wind direction. An empirical relation for Goodnoe Hills was established based on a linear regression of I_V measurements obtained from a uvw anemometer under a variety of conditions with measurements of wind direction fluctuations taken from the wind vanes at the BPA and PNL towers. As a result:

$$B = 0.01468 + 4.1091I_V \text{ (for } I_V > 0.04) \qquad (5.6)$$

$$B = 0.18 \text{ (for } I_V < 0.04) \quad .$$

The Lissaman and simplified wake models were run to obtain centerline velocity deficits under conditions where the turbine C_p is a maximum (C_T = 0.43 at a tip speed ratio of 8.4 from Figure 5.3). The incident wind speed is 22 mph. The models were calculated for transverse turbulence intensities ranging from 0.05 to 0.12. Turbine power ratios were converted to velocity ratios using Equation (5.2).

The results of the model calculations, along with the measured values, are shown in Table 5.1. As stated earlier, a natural discrepancy, although small, is apparent in the background measurements at the two meteorological towers. An even greater discrepancy in background values between turbines #1 and #3 has also been observed. This discrepancy is accounted for in the measured values shown in Table 5.1, but direct comparison against the model results should be treated with caution. In addition, and perhaps even more importantly, the measured values represent an ensemble of meteorological conditions, whereas the model values represent two specific sets of meteorological conditions. Nevertheless, the comparison with both the simplified wake model and the Lissaman model is rather good, particularly for the higher turbulence intensities values. It is also of interest to note that, except in the near-wake region, the simplified and Lissaman models produce nearly identical results.

TABLE 5.1. Velocity Ratios Calculated From the Modified Lissaman and Simplified Wake Models for Two Turbulence Intensity (T_V Values and Maximum Rotor Thrust (C_T = 0.43), and the Measured Results for Tip Speed Ratio at Maximum C_p

		Velocity Ratios				
Wake Combination	Downwind Distance	Modified Lissaman T1 = 0.05	Modified Lissaman T1 = 0.12	Simplified Wake T1 = 0.5	Simplified Wake T1 = 0.12	Measured
T1 on PNL	2.2 dia	0.56	0.64	0.74	0.74	0.66
T2 on T1	6.7 dia	0.76	0.89	0.78	0.87	0.85
T3 on PNL	8.3 dia	0.79	0.90	0.80	0.89	0.92
T3 on T1	10.2 dia	0.83	0.93	0.83	0.91	1.01

5.3 COMPARISON WITH PREVIOUS STUDIES AT GOODNOE HILLS

Hadley and Renne (1983) summarized the results of three field experiments conducted during the summer of 1982 at Goodnoe Hills to characterize the wake of a MOD-2 under a variety of conditions. One study (Liu et al. 1983) used visual tracer techniques to obtain quantitative characteristics of the wake out to about 5 D. A second study (Lissaman, Gyatt and Zalay 1982) used a tethered balloon sonde system to obtain velocity deficit profiles near the wake centerline. In a third study, Baker and Walker (1983) used kite anemometers to obtain two- and three-dimensional patterns of the wake at downwind distances out to 9 D.

Hadley and Renne (1983) drew a composite structure of the wake, including centerline velocity deficits, based on these three studies. This composite is shown in Figure 5.6. Included in this figure is information on the velocity deficit based on the analysis of machine/machine and machine/tower interaction data provided here. (Hadley and Renne's report provided some initial results of these same data). As can be seen, the results of this analysis are consistent with the findings of the investigators during the summer of 1982.

As with the findings reported here, the investigators found reasonable agreement with the modified Lissaman model, although Liu et al. (1983) conclude that the model overpredicts wake radius growth and downwind momentum deficits, while Lissaman, Gyatt and Zalay (1982) generally conclude that the model

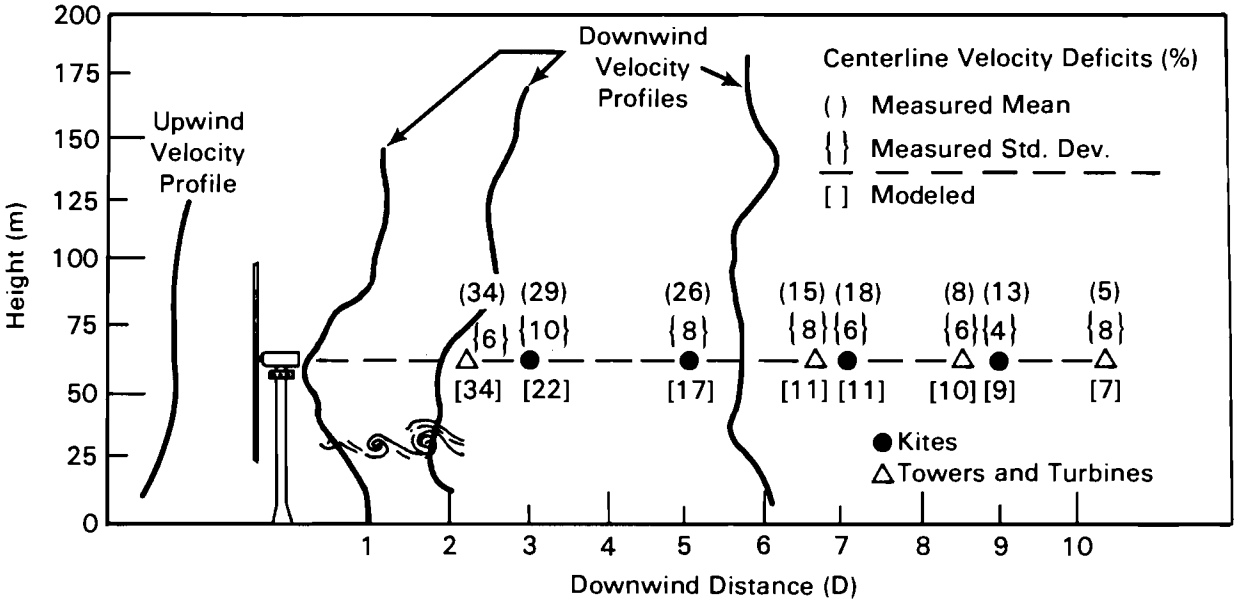

FIGURE 5.6. Composite Representation of the Results of the Wake Measurements Program at Goodnoe Hills (Hadley and Renne 1983)

underpredicts these values. However, the scatter in the measurements makes precise verification of the models impossible with these studies.

The three investigators all observed an asymmetry to the wake structure, similar to that noted in Chapter 4 of this report, downwind of turbine #3. They attributed this to terrain-induced variability on the flow. This wake asymmetry was not observed downwind of turbine #1, which would rule out rotor-induced wake asymmetry in the far-wake region.

6.0 CONCLUSIONS AND RECOMMENDATIONS

6.1 CONCLUSIONS FROM OBSERVATION AND ANALYSIS OF DATA

The following conclusions on wind turbine wake characteristics can be drawn from analysis of the August 29 to November 12, 1982, data set collected at the Goodnoe Hills MOD-2 array.

- Based on turbine power output measurements, power deficits of a downstream MOD-2 in the wake of an upstream MOD-2 average about 24% at a downwind distance of 6.7 D (rotor diameters) and 14% at a downwind distance of 10.2 D. A rotor diameter is 300 ft.
- Based on measurements at the two meteorological towers, velocity deficits in the wake average 25% at 2.2 D downwind and 15% at 8.3 D downwind of a MOD-2.
- The composite wake structure at a given measurement location indicates some cross-wake asymmetry, a result of either terrain influences or instrument error. A slight curvature in the wake trajectory is also observed for some cases, particularly at lower incident wind speeds.
- The average of the measurements at 2.2 D downwind indicates that near-wake characteristics usually prevail at this distance. Far-wake conditions appear to prevail at all other downwind measurement distances.
- Maximum power (and velocity) deficits occur at a tip speed ratio of around 8, which is near the maximum operational C_p and C_T values of the MOD-2. At other tip speed ratios, the wake recovers more rapidly.
- The magnitude of the far wake is less for higher ambient turbulence intensities.
- A slight increase in the turbulence of the wake is observed at the 200- and 350-ft levels, but not at the 50-ft level.
- These results do not change when different time averaging is used in the data analysis.

- There is good comparison between the averaged velocity deficits and those calculated by the modified Lissaman and simplified wake models, particularly for higher ambient turbulence intensities.

6.2 RECOMMENDATIONS FOR FUTURE WORK

A serious shortcoming with the data collected during the August 29 to November 12, 1982, period is the lack of information at some of the important separation distances between turbines or between a turbine and a tower. If data were available at these distances a more comprehensive characterization of the wake, and the transition from near-wake to far-wake characteristics, could be obtained. These would include interactions between turbines #2 and #3 (5.0 D), turbines #1, #2, and #3 on the BPA tower (9.0, 3.3, and 1.7 D, respectively), and turbine #2 on the PNL tower (5.8 D). Another shortcoming of the data set is that only limited meteorological conditions are represented. There are no data available for the windiest periods at the site, which occur in the spring. As a result, we strongly recommend that this measurement program be continued when at least pairs of machines are operating, so that a data set of sufficient duration can be obtained to develop wakes information at all these downwind distances for a variety of meteorological conditions.

We also recommend that individual case studies of machine/machine or machine/tower wake interactions be evaluated in more detail. This could be done by creating special data sets that include all fifty parameters monitored by the DDS for specific case periods, so that additional information on the wake could be analyzed.

Finally, we recommend that comparison of the results against various numerical models be continued, so that the models can be refined to reflect actual measurements around full-scale turbines. This could lead to improved methods of evaluating the performance efficiency of an array of wind turbines, and could lead to better guidelines for evaluating a site and for spacing wind turbines within an array.

7.0 REFERENCES

Abramovich, G. N. 1963. The Theory of Turbulent Jets. MIT Press, Cambridge, Massachusetts.

Ainslie, J. F. 1981. Computer Modeling of Clusters of Wind Turbines. RD/L/N 187/80, Central Electricity Research Laboratories, England.

Ainslie, J. F. 1982. Comparison of Wake Models for Computing Interactive Effects Between Wind Turbines. TPRD/L/2302/N82, Central Electricity Research Laboratories, England.

Ainslie, J. F. 1983. Development of an Eddy Viscosity Model of a Wind Turbine Wake. TPRD/L/AP/0081/M83, Central Electricity Generating Board, England.

Alfredsson, P. H., J. A. Dahlberg and F. H. Bark. 1980. "Some Properties of the Wake Behind Horizontal Axis Wind Turbines." Paper presented at Third International Symposium on Wind Energy Systems, sponsored by BHRA Fluid Engineering, Cranfield, Bedford, England.

Baker, R. W. and S. N. Walker. 1982. Wake Studies at the Goodnoe Hills MOD-2 Site. Oregon State University, Corvallis, Oregon.

Connell, J. R. and R. L. George. 1982. The Wake of the MOD-0A1 Wind Turbine at Two Rotor Diameters Downwind on December 3, 1981. PNL-4210, Pacific Northwest Laboratory, Richland, Washington.

Crafoord, C. 1979. Interaction in Limited Arrays of Windmills. Report DM-26, University of Stockholm, Stockholm, Sweden.

de Vries, O. 1979. Fluid Dynamic Aspects of Wind Energy Conversion. AGARD-AG-243, National Aerospace Laboratory NLR, Amsterdam, The Netherlands.

Doran, J. C. and K. R. Packard. 1982. Comparison of Model and Observations of the Wake of a MOD-0A Wind Turbine. PNL-4433, Pacific Northwest Laboratory, Richland, Washington.

Eberle, W. R. 1981. Wind Flow Characteristics in the Wakes of Large Wind Turbines. Volume 1 - Analytical Model Development. DOE/NASA/0029-1. U.S. Department of Energy, Washington, D.C.

Hadley, D. L. and D. S. Renne. 1983. "Wake Research in the Federal Wind Energy Program." In Proceedings, ASES '83 Annual Meeting and Wind Workshop VI, June 1983, American Solar Energy Society, Boulder, Colorado.

Lissaman, P.B.S. 1977. Energy Effectiveness of Arrays of Wind Energy Collection Systems. AVR 6110, Aerovironment, Inc., Pasadena, California.

Lissaman, P.B.S. and E. R. Bate. 1977. Energy Effectiveness of Arrays of Wind Energy Conversion Systems. AVFR 7058, Aerovironment, Inc., Pasadena, California.

Lissaman, P.B.S. 1979. Energy Effectiveness of Arbitrary Arrays of Wind Turbines. AIAA Paper No. 79-0114, AIAA, New York.

Lissaman, P.B.S., G. W. Gyatt and A. D. Zalay. 1982. Numerical Modeling Sensitivity Analysis of the Performance of Wind Turbine Arrays. PNL-4183, Pacific Northwest Laboratory, Richland, Washington.

Liu, H.-T., J. W. Waite, T. R. Hiester, P. H. Tacheron and R. A. Srnsky. 1983. Flow Visualization Study of the MOD-2 Wind Turbine Wake. PNL-4535, Pacific Northwest Laboratory, Richland, Washington.

Miller, A. H., H. L. Wegley, and J. W. Buck. 1984. "Large HAWT Wake Measurement and Analysis." Paper presented at the DOE/NASA Wind Turbine Technology Workshop, May 8-10, 1984, Cleveland, Ohio.

Riley, J. J., E. W. Geller, M. D. Coon and J. C. Schedvin. 1980. A Review of Wind Turbine Wake Effects. DOE/ET/23160-80/1, National Technical Information Service, Springfield, Virginia.

Sforza, P. M., W. Stasi, M. Smorto and P. Sheerin. 1979. Wind Turbine Generator Wakes. AIAA Paper No. 79-0113, AIAA, New York.

Tennekes, H. and J. L. Lumley. 1972. A First Course in Turbulence. MIT Press, Cambridge, Massachusetts.

Vermuelen, P. 1978. A Wind Tunnel Study of the Wake of a Horizontal-Axis Wind Turbine. TNO Report 78-09674, Organization for Industrial Research, The Netherlands.

Vermeulen, P.E.J. and P.J.H. Builtjes. 1981. Mathematical Modeling of Wake Interaction in Wind Turbine Arrays. Part 1, TNO Report 81-01473, Organization for Industrial Research, The Netherlands.

Walker, S. N. and P.B.S. Lissaman. 1978. Wind Flow Characteristics in the Wake of Large Wind Turbines. AVFR 8147, Aerovironment, Inc., Pasadena, California.

Wilson, R. E., P.B.S. Lissaman, and S. N. Walker. 1976. Aerodynamic Performance of Wind Turbines. ERDA/NSF/04014-76/1, National Technical Information Service, Springfield, Virginia.

Wilson, R. E. and P.B.S. Lissaman. 1974. Applied Aerodynamics of Wind Power Machines. Oregon State University, Corvallis, Oregon.

DISTRIBUTION

No. of Copies

OFFSITE

Carl Aspliden
Battelle Memorial Institute
Washington Office
2030 M Street NW
Washington, DC 20036

J. Cadogan
Department of Energy
Wind Energy Technology Division
1000 Independence Avenue
Forrestal Building, Room 5H048
Washington, DC 20585

D. F. Ancona
Department of Energy
Wind Energy Technology Division
1000 Independence Avenue
Forrestal Building, Room 5H048
Washington, DC 20585

G. P. Tennyson
Department of Energy
Albuquerque Operations Office
P.O. Box 5400
Albuquerque, NM 87110

30 DOE Technical Information Center

Peter Lissaman
Aerovironment, Inc.
145 Vista Avenue
Pasadena, CA 91107

Tom Gray
American Wind Energy Association
1516 King Street
Alexandria, VA 22314

W. A. Vachon
P.O. Box 149
Manchester, MA 01944

No. of Copies

Mike Bovarnick
Boeing Aerospace Corporation
P.O. Box 3999
Seattle, WA 98124

Wayne Wiesner
Boeing Aerospace Corporation
P.O. Box 3999
Seattle, WA 98124

Gary Miller
Boeing Aerospace Corporation
P.O. Box 3999
Seattle, WA 98124

Mike Rees
Boeing Aerospace Corporation
PO Box 3999
Seattle, WA 98124

Don Fries
Boeing Aerospace Corporation
P.O. Box 3999
Seattle, WA 98124

Dick Hacker
Boeing Aerospace Corporation
P.O. Box 3999
Seattle, WA 98124

Ron Holeman
Bonneville Power Administration
Generation Engineering
P.O. Box 3621
Portland, OR 97208

S. J. Hightower
Bureau of Reclamation
Denver Federal Center
Building 67, Code 254
Denver, CO 80225

Willi Sadeh
Department of Civil Engineering
Colorado State University
Fort Collins, CO 80523

No. of Copies

V. A. Sandborn
Department of Civil Engineering
Colorado State University
Fort Collins, CO 80523

Dr. Edgar DeMeo
Electric Power Research Institute
3412 Hillview Avenue
Palo Alto, CA 94303

Frank Goodman, Jr.
Electric Power Research Institute
3412 Hillview Avenue
Palo Alto, CA 94303

R. L. George
TERRA Sciences, Inc.
7555 W. 10th Avenue
Lakewood, CO 80214

Tom Hiester
FloWind Corporation
1183 Quarry Lane
Pleasanton, CA 94566

J. M. Kos
Hamilton Standard
Bradley Field Road
Windsor Locks, CT 06096

Eugene Di Valentin
Hamilton Standard
Bradley Field Road
Windsor Locks, CT 06096

Glid Doman
Hamilton Standard
Bradley Field Road
Windsor Locks, CT 06096

G. L. Park
Department of Electrical Engineering
Michigan State University
East Lansing, MI 48824

No. of Copies

R. B. Schlueter
Department of Electrical Engineering
Michigan State University
East Lansing, MI 48824

W. D. Johnston
Hawaiian Electric Company, Inc.
P.O. Box 2750
Honolulu, HI 96840

David Spera
NASA/Lewis Research Center
21000 Brookpark Road
Cleveland, OH 44135

Phillip French
NASA Scientific and Technical Information Facility
P.O. Box 8757
Baltimore/Washington International Airport
Baltimore, MD 21240

J. C. Kaimal
National Oceanic and Atmospheric Administration/Environmental Research Laboratories/Wave Propagation Laboratory
3000 Marine Street
Boulder, CO 80302

G. M. Gregorek
Aeronautics and Astronautics Research Lab
Ohio State University
2300 W. Case Road
Columbus, OH 43220

Peter M. Moretti
Oklahoma State University
Mechanical and Aerospace Engineering
Engineering North 218
Stillwater, OK 74074

No. of
Copies

Robert Wilson
Department of Mechanical
Engineering
Oregon State University
Corvallis, OR 97331

Dr. H. A. Panofsky
6222 Agee Street #5
San Diego, CA 92122

J. Dutton
Department of Meteorology
Pennsylvania State University
University Park, PA 16902

Andrew Trenka
Solar Energy Research Institute
Rocky Flats
P.O. Box 464
Golden, CO 80401

P. Klimas
Sandia Laboratories
Division 5443, P.O. Box 5800
Albuquerque, NM 87115

Robert Noun
Solar Energy Research Institute
1617 Cole Boulevard
Golden, CO 80401

Robert Thresher
Solar Energy Research Institute
1617 Cole Boulevard
Golden, CO 80401

Sherman M. Chan
Systems Control, Inc.
1801 Page Mill Road
P.O. Box 10025
Palo Alto, CA 94303

R. H. Kirchhoff
Department of Mechanical
Engineering
University of Massachusetts
Amherst, MA 01003

No. of
Copies

Earl L. Davis
U.S. Windpower, Inc.
2305 S. Vasco Road
Livermore, CA 94550

H. Tieleman
Department of Engineering Science
& Mechanics
Virginia Polytechnic Institute and
State University
Blacksburg, VA 24061

Susan Hosch
Washington State Energy Office
400 E. Union Avenue, 1st Floor
Olympia, WA 98504

Farrell Smith Seiler
Wind Energy Report
Box 14 - 104 S. Village Avenue
Rockville Centre, NY 11571

FOREIGN

Leif Kristensen
Department of Physics
Risø National Laboratory
4000 Roskilde
DENMARK

Per Lundsager
Risø National Laboratory
P.O. Box 49
DK-4000 Roskilde
DENMARK

Dr. M. B. Anderson
Sir Robert McAlpine & Sons, Ltd.
40 Bernard Street
London WC1N 1LG
ENGLAND

Dr. D. Wilson
Cavendish Laboratory
Madingley Road
Cambridge CB3 OHE
ENGLAND

No. of
Copies

D. Lindley
Taylor Woodrow Construction, Ltd.
Taywood House
345 Ruislip Road
Southall
Middlesex UBI 2QX
ENGLAND

Dr. Neil Cherry
Lincoln College
Canterbury
NEW ZEALAND

ONSITE

DOE Richland Operations Office

H. E. Ransom/D. R. Segna

39 Pacific Northwest Laboratory

J. W. Buck (5)
J. R. Connell
D. W. Dragnich
C. E. Elderkin
D. L. Elliott
J. M. Hales
P. C. Hays
M. E. Hinchee
B. D. Holst
A. H. Miller
V. R. Morris
E. L. Owczarski
D. C. Powell
D. S. Renne (5)
J. A. Stottlemyre
T. K. Thompson
R. E. Wildung
H. L. Wegley
L. L. Wendell
Technical Information Files (5)
Publishing Coordination (2)
WCPE Program Office (5)